Vegetation uptake of mercury and impacts on global cycling

Jun Zhou[1,4]✉, *Daniel Obrist*[1,4]✉, *Ashu Dastoor*[2], *Martin Jiskra*[3] *and Andrei Ryjkov*[2]

Abstract | Mercury (Hg) is a global pollutant that emits in large quantities to the atmosphere (>6,000–8,000 Mg Hg per year) through anthropogenic activities, biomass burning, geogenic degassing and legacy emissions from land and oceans. Up to two-thirds of terrestrial Hg emissions are deposited back onto land, predominantly through vegetation uptake of Hg. In this Review, we assemble a global database of over 35,000 Hg measurements taken across 440 sites and synthesize the sources, distributions and sinks of Hg in foliage and vegetated ecosystems. Lichen and mosses show higher Hg concentrations than vascular plants, and, whereas Hg in above-ground biomass is largely from atmospheric uptake, root Hg is from combined soil and atmospheric uptake. Vegetation Hg uptake from the atmosphere and transfer to soils is the major Hg source in all biomes, globally accounting for 60–90% of terrestrial Hg deposition and decreasing the global atmospheric Hg pool by approximately 660 Mg. Moreover, it reduces the Hg deposition to global oceans, which, in the absence of vegetation, might receive an additional Hg deposition of 960 Mg per year. Vegetation uptake mechanisms need to be better constrained to understand vegetation cycling, and model representation of vegetation Hg cycling should be improved to quantify global vegetation impacts.

Minamata Convention on Mercury
An international treaty named after the city of Minamata in Japan that experienced devastating Hg contamination in the 1950s.

[1]*Department of Environmental, Earth and Atmospheric Sciences, University of Massachusetts Lowell, Lowell, MA, USA.*

[2]*Air Quality Research Division, Environment and Climate Change Canada, Dorval, Quebec, Canada.*

[3]*Environmental Geosciences, University of Basel, Basel, Switzerland.*

[4]*These authors contributed equally: Jun Zhou, Daniel Obrist.*

✉*e-mail: jun_zhou@uml.edu; daniel_obrist@uml.edu*

https://doi.org/10.1038/s43017-021-00146-y

Mercury (Hg) is a globally abundant pollutant found in all major environmental reservoirs. Hg is mainly distributed through the atmosphere[1], transporting Hg from emission sources (such as industrial centres) to remote aquatic and terrestrial ecosystems[1–3]. Thus, in 2013, the Minamata Convention on Mercury was signed to curb anthropogenic Hg emissions and to reduce Hg risks to humans and the environment[4]. In 2015, an estimated 2,000–3,000 Mg per year of Hg was emitted to the atmosphere by anthropogenic activities[5]. Approximately, an additional 200–600 Mg per year of Hg is emitted through biomass burning[6–8], with another 1,000–1,600 Mg per year through terrestrial geogenic emissions[8] and legacy emissions from soils and vegetation[6,8–10]. Indeed, legacy emissions are now considered to dominate global Hg emissions to the atmosphere, mostly emitted over oceans (about 2,700–3,400 Mg per year)[6,8–11].

In terrestrial ecosystems, the dominant source of Hg is related to vegetation assimilation of atmospheric Hg and subsequent transfer to soils and watersheds through the washing of vegetation by precipitation (throughfall); when vegetation sheds leaves (litterfall)[12,13]; or when vegetation dies off. Additionally, plant roots take up Hg from soils, which impacts soil Hg availability and stabilizes Hg below ground (referred to as phytostabilization)[14–16]. Hg-contaminated soils have the potential to lead to enhanced Hg levels in crops and rice plants, so that control and remediation of contaminated sites is an important step to increase food safety[17].

Recognition of the critical importance of vegetation for terrestrial Hg cycling began in the 1990s, when it was found that litterfall and throughfall Hg deposition in forests exceeded direct open-field wet deposition (by rain and snow) severalfold[12,13,18–20]. Since these early studies, it has been shown that vegetation impacts Hg cycling in all major Earth system compartments. For example, field deposition studies show that plant-derived deposition dominates as a Hg source in ecosystems with high plant net primary productivity[21]. Atmospheric observations indicate that vegetation uptake of atmospheric Hg(0) — the gaseous, elemental and dominant type of Hg (>95%) in the atmosphere — modulates both its seasonality and concentrations in the boundary layer[22,23]. Moreover, soil and sediment studies show that vegetation shapes Hg loads across landscapes, with densely vegetated ecosystems and productive watersheds exhibiting the highest Hg loads[24–29]. Hg assimilated by vegetation is subsequently exported from watersheds via streams[30–34], where it can dominate as a source of Hg in rivers and ocean sediments[35,36], and is found to bioaccumulate in fish[37–39].

In this Review, we discuss Hg uptake by vegetation and its impact on global Hg cycling. We compile published Hg concentration data in vegetation tissue from 440 sites into a global database and analyze Hg distribution

Key points

- In forest ecosystems, 60–90% of mercury (Hg) originates from vegetation uptake of atmospheric gaseous elemental mercury (Hg(0)), providing 1,180–1,410 Mg per year of terrestrial Hg deposition.
- Vegetation uptake of atmospheric Hg(0) lowers the global atmospheric Hg burden by 660 Mg and reduces deposition to global oceans, which would receive an additional Hg deposition of 960 Mg per year without vegetation.
- Lichen and mosses show higher Hg concentrations than vascular plants, and, whereas Hg in above-ground biomass is largely from atmospheric uptake, root Hg is from combined soil and atmospheric uptake.
- The seasonality of atmospheric Hg(0) concentrations in the Northern Hemisphere is controlled by vegetation uptake. Simulations without vegetation show weak seasonal cycles and cannot reproduce observations.
- Large knowledge gaps exist in understanding physiological and environmental controls of vegetation Hg uptake and transport within plants, limiting our mechanistic and molecular-level understanding of vegetation Hg uptake.
- Improved model parameterizations and harmonized observational data of vegetation Hg uptake, along with whole-ecosystem Hg(0) exchange measurements, are needed to improve the assessment of vegetation impacts on global Hg cycling.

patterns across ecosystem types, plant functional groups and plant tissues. We describe Hg uptake, transport within plants and isotopic fractionation; foliage–atmosphere exchange of Hg; and the representation of vegetation Hg dynamics in global models. The importance of vegetation uptake in atmospheric Hg fluxes is examined and further research priorities are detailed.

Hg in vegetation

To understand Hg dynamics in vegetation globally, we built a comprehensive database by collecting peer-reviewed published data on Hg concentrations measured in vegetation tissues. Data stretch from 1976 to 2020 and include 440 different sites, derive from 230 scientific studies and consist of 2,490 reported data representing over 35,000 individual plant tissue measurements (Supplementary Information). Hg concentrations are separated into different tissue groups (including leaves, needles, roots, woody tissues including bole wood, bark and branches), plant functional types (including lichens, mosses and vascular plants such as grassland plants, shrubs and trees), species and geographic areas (FIG. 1). Currently available vegetation data are unevenly distributed globally (FIG. 1a, Supplementary Fig. 1), with most foliage and litterfall measurements taken in Europe (46.6%), followed by North America (23.0%), Asia (17.2%) and South America (13.1%). Most vegetation data stem from deciduous trees (77.9%) and coniferous trees (9.1%), whereas evergreen broadleaved trees (4.8%), grasslands (4.3%) and wetlands (3.9%) have been sampled less (FIG. 1b). Foliar data, which include leaves, needles and litterfall, represent about 78% of all available data (FIG. 1c). Less data are available from woody tissues, branches, bark and grassland plants, which, even combined, account for less than 9.8% of the data (FIG. 1c).

Foliage and litterfall Hg concentrations were highest in South America, followed by Europe and Asia, and were lowest in North America, with similar spatial patterns observed amongst the other tissues (FIG. 1a, Supplementary Fig. 2). Differences were pronounced in some tissues, with foliage Hg concentrations in South America (median: 54 $\mu g\,kg^{-1}$ [interquartile range (IQR): 8–123 $\mu g\,kg^{-1}$]) more than double the concentrations in North America (20 $\mu g\,kg^{-1}$ [3–41 $\mu g\,kg^{-1}$]). However, owing to large differences in investigated forest types, non-random sampling procedures and some studies including regional (natural or anthropogenic) Hg contamination hotspots (BOX 1), spatial comparisons are likely to be biased. Across unpolluted areas, median Hg concentrations derived from our database across functional groups and vegetation tissues varied in the following order: lichen (median: 78 $\mu g\,kg^{-1}$, [IQR: 10–180 $\mu g\,kg^{-1}$]) > moss (51 $\mu g\,kg^{-1}$ [2–165 $\mu g\,kg^{-1}$]) > litterfall (43 $\mu g\,kg^{-1}$ [4–83 $\mu g\,kg^{-1}$]) > foliage (20 $\mu g\,kg^{-1}$ [2–62 $\mu g\,kg^{-1}$]) > bark (11 $\mu g\,kg^{-1}$ [1–36 $\mu g\,kg^{-1}$]) > branch (12 $\mu g\,kg^{-1}$ [0.2–37 $\mu g\,kg^{-1}$]) > root (7 $\mu g\,kg^{-1}$ [2–70 $\mu g\,kg^{-1}$] > grass (5 $\mu g\,kg^{-1}$ [1–31 $\mu g\,kg^{-1}$]) > wood (2 $\mu g\,kg^{-1}$ [0.1–6.8 $\mu g\,kg^{-1}$]) (FIG. 1c). A similar order of Hg concentrations was observed for vegetation grown in polluted areas (BOX 1; Supplementary Fig. 2). In this section, we discuss detailed pathways and mechanism of Hg uptake and transport behaviour within vegetation that explain these observed concentration patterns.

Vascular plants. Vascular plants uptake Hg through stomatal and cuticular uptake in foliage[40–42], surface adsorption of atmospheric Hg to foliage[43] and bark[40,44], and soil uptake of Hg through roots[42,45–48] (FIG. 2). There is strong evidence that most Hg originates from assimilation of atmospheric uptake in above-ground tissues[49]. Many lines of evidence, including from flux measurements[50–53] and stable Hg isotope analyses[54–61], show that approximately 90% of Hg in leaves and needles is derived from atmospheric uptake of gaseous Hg(0) and that translocation of Hg from soils to above-ground tissues is limited. For example, 11% of Hg in a canopy originated from soils via xylem transport in boreal trees[62] and less than 5% of soil solution root Hg uptake was translocated to shoots in a variety of different plant species[42,56,63]. Most leaf Hg (90–96%) is integrated into internal tissues[48] and a only minor part adsorbed to outer leaf surfaces[61].

Inside leaves, Hg is incorporated in epidermal and stomatal cell walls, as well as in parenchyma cell nuclei[64] (FIG. 2). This Hg is present as divalent Hg(II), so there must be an oxidation step after leaf uptake of Hg(0), although it is currently unknown where and when the oxidation step occurs. Both stomatal and non-stomatal uptake pathways in leaves have been proposed, although several studies point towards a dominance of stomatal uptake[48,49,53,61,65], based on isotopically labelled Hg(0) exposures[61,64,66], natural abundant Hg stable isotopes[57,58], sequential leaf extractions[48,67] and foliage–atmosphere exchange studies[43,68]. However, observed Hg(0) uptake at night also suggests that non-stomatal, cuticular Hg(0) uptake occurs[69–71]. Stomatal Hg(0) uptake is likely controlled by enzymatic processes (such as catalase activity), which has also been linked to Hg oxidation in leaves[67]. Hg species stored in leaves include sulfur nanoparticulate (β-HgS) and dithiolate complexes ($Hg(SR)_2$)[72], and Hg binding to thiol ligands such as cysteine residues[73,74].

Concentrations of Hg in vascular plants are highest in leaves and needles (FIG. 1c), and, because Hg is taken up from the atmosphere, these concentrations are highly

Legacy emissions
Re-volatilization of past atmospheric deposition from anthropogenic and geogenic sources stored in surface reservoirs, such as soils and water.

Vascular plants
Group of plants with specialized tissues that include coniferous and flowering plants.

Stomata
Apertures in leaves that control gas exchange (such as carbon dioxide and water vapour) between plants and the atmosphere.

Cuticles
Outer protective layers on epidermal cells of leaves, often consisting of waxy, water-repellent substances.

sensitive to variations in atmospheric Hg concentrations. Growth chamber and laboratory studies have shown that atmospheric Hg(0) concentrations linearly and positively correlate with Hg concentrations in shoots, leaves and needles[14,49,51–53,75,76]. Similarly, field observations show significant positive correlations between Hg(0) concentrations in the atmosphere and foliage[72,77]. Based on our global database, we observed a significant positive linear correlation between leaf and needle Hg concentrations and atmospheric Hg concentrations across unpolluted sites ($n = 33$, $r^2 = 0.32$, $P < 0.01$; Supplementary Fig. 3).

Other factors have been associated with variability in Hg accumulation in foliage, including underlying geology[78], solar radiation (in particular, ultraviolet)[79], temperature[80], atmospheric turbulence[81], leaf age[57,82], specific leaf area[48,53], number of stomata[48] and leaf physiological parameters, such as stomatal conductance[43,68], rate of net photosynthesis[83], the presence of waxy cuticles[84], catalase activity[85] and ascorbic acid[86]. Many of these processes can be linked to stomatal control of Hg uptake (such as stomatal conductance, number of stomata, catalase activity), whereas others can be linked

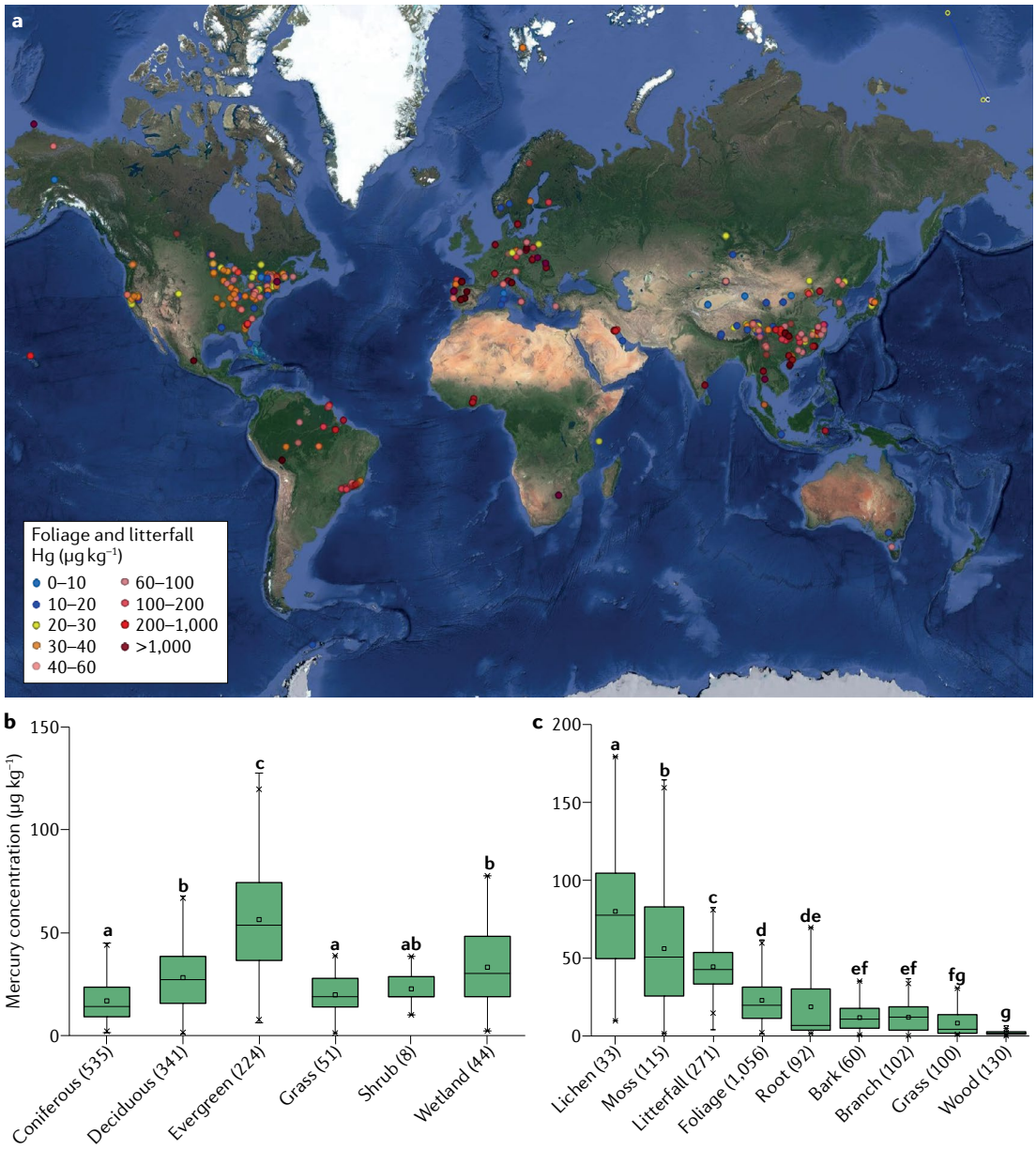

Fig. 1 | **Global distribution of foliar Hg samples. a** | Spatial coverage of foliar and litterfall mercury (Hg) samples from the database compiled here, including both background and Hg-enriched areas, with concentration averaged by site. **b** | Box plots of Hg concentrations of foliage in background sites separated by biomes and/or plant community types. **c** | Box plots of Hg concentrations for various tissue types from background sites. Numbers in parentheses represent the number of data points per group. Boxes represent quartile ranges, lines mark medians and squares mark means. Whiskers show minimum and maximum values, and stars denote 1st and 99th percentiles. Different letters represent statistical differences among groups ($P < 0.05$). Corresponding data for Hg-enriched sites are shown in Supplementary Fig. 2a.

Non-vascular vegetation
Plants that do not have specialized vascular tissues, which include algae, mosses, livermorts and hornworts; lichen are often grouped into this category, although they are symbiotic partnerships between a fungus and an alga.

to non-stomatal uptake pathways (such as waxy cuticles and specific leaf area). Hg concentrations in foliage have been consistently shown to increase with leaf age, both over a growing season[48,87] and over multiple years in coniferous needles[88–90]. Higher concentrations have been reported in evergreen coniferous tissues than in broadleaf trees, owing to the multi-year lifetime of coniferous needles[47,91,92]. When comparing foliage of the same age, however, coniferous needles exhibit lower Hg concentrations than deciduous leaves, which is attributed to a lower metabolic activity of needles[87] and is consistent with reduced deposition on needles, as observed using dynamic flux bag measurements[53,55,57,80,82,93]. Although in our database we cannot account for leaf age, we, indeed, find significantly higher Hg concentrations in deciduous leaves (median: 28 $\mu g\,kg^{-1}$ [IQR: 2–70 $\mu g\,kg^{-1}$]) compared with coniferous needles (15 $\mu g\,kg^{-1}$ [2–47 $\mu g\,kg^{-1}$]), and the highest concentrations in tropical broadleaf evergreen leaves (56 $\mu g\,kg^{-1}$ [7–131 $\mu g\,kg^{-1}$]) (FIG. 1b).

In addition to varying amongst foliage, concentrations of Hg vary among woody tissues (FIG. 1c). The outermost bark, characterized by a high porosity and relative chemical inertness, lacks metabolic processes and, thus, likely absorbs airborne Hg via non-physiological adsorption processes[40,44]. Across the bark, Hg concentrations markedly decrease from the outermost to the innermost layers (including the phloem)[94], indicating little transport through the bark. Potential pathways for Hg in bole wood include root uptake and translocation through the xylem, foliage uptake and translocation by phloem transport, and transfer from the bark (FIG. 2). However, Hg uptake to bole wood, which is the tissue showing by far the lowest Hg concentrations (FIG. 1c; Supplementary Fig. 2), is considered to be dominated by translocation of foliage Hg to tree rings through phloem transport, whereas transport through translocation from roots and bark is likely negligible[40–42]. Notably, this transport could enable the use of tree ring Hg to track historic, local, regional and global Hg exposures[40,41,94–102].

Below ground, plant roots and excretions (chelators) can induce pH variations and redox reactions in soils, which, subsequently, lead to cation exchange of divalent Hg and solubilization of Hg from nearly insoluble soil Hg precipitates[103,104] (FIG. 2). Hg then likely penetrates into root cells as a hitch-hiker using transporters for other elements[105,106], as Hg is a non-essential element. Absorbed Hg is largely restricted to the cell walls of the outer layers of the root cortical cylinder, as well as to the central cylinder and parenchyma cell nuclei[64]. Accumulation in root cells can reduce the movement of Hg from the root into the xylem, and transport of Hg–phytochelatin complexes into vacuoles can restrict phloem mobility[106,107]. Low Hg translocation from soils to above-ground tissues has been attributed to effective Hg retention in roots[108]. However, no specific transport molecules involved in Hg uptake by roots and translocation in roots are known.

Root Hg concentrations have been shown to linearly correlate with soil concentrations[14,75,109] and show low sensitivity to air Hg concentrations[14], leading to the view that Hg in roots is derived primarily from soil uptake. However, exceptions have been reported in quaking aspen[76] and wheat[14,53] under very high atmospheric Hg exposures (20–40 times ambient air concentrations). Moreover, stable Hg isotope studies have pointed to contrasting Hg origins in roots. For example, rice plants grown in contaminated soils showed root Hg with the same isotopic signature as the surrounding soil[110], indicating root uptake. In contrast, substantial foliage-to-root Hg transport was observed in a forest, where atmospheric Hg(0) uptake via foliage accounted for 44–83% of Hg in tree roots[111]. In the latter study, large roots showed somewhat higher proportions of atmospheric Hg(0) compared with small roots (59% versus 64%)[111], possibly related to lower surface areas and reduced absorptive potential of large roots[108,112]. The role of atmospheric uptake in root Hg merits further detailed investigations, as this phenomenon would substantially increase estimates of plant Hg uptake from the atmosphere due to high turnover rates of roots, which could equal that of leaf litterfall[108].

Non-vascular vegetation. Non-vascular vegetation, including lichens and mosses (slow-growing cryptogamic organisms without root systems or thick waxy cuticles), generally show much higher Hg concentrations

Box 1 | **The role of vegetation in Hg-enriched areas**

In addition to anthropogenic mercury (Hg) contamination from urban and industrial, mining or smelting sites, natural Hg enrichments exist on the global mercuriferous belts found along Earth plate margins, leading to large-scale Hg mineralization zones: Circum-Pacific, Mediterranean, Central Asia and Mid-Atlantic ridges, with many Hg mines distributed along these zones[250]. When exposed to high soil and atmospheric Hg levels, plant growth can be decreased due to Hg toxicity[251–254]. However, most plants grow normally under lightly to moderately polluted areas, but will show substantial Hg enrichments in their tissues. In comparison with remote, non-enriched sites, median Hg concentrations of vegetation from Hg-enriched areas in our database show significantly higher Hg concentrations ($P < 0.01$) by factors of 1.2–5.7 across all tissues. Specific tissue responses are dependent on the type of exposure, with soil Hg contamination resulting largely in elevated root Hg concentrations, while not significantly affecting above-ground tissue concentrations. In turn, atmospheric Hg contamination significantly elevates Hg levels in above-ground Hg concentrations ($P < 0.01$) but did not impact below-ground tissues.

The potential use of plant Hg uptake has received interest as an alternative method for traditional physico-chemical methods of remediation of Hg-enriched sites, termed phytoremediation. In summary, there are three main approaches of Hg phytoremediation: phytostabilization, phytovolatilization and phytoextraction. Phytostabilization immobilizes Hg in soil through biochemical processes, either via Hg accumulation in roots or chelating Hg in the root zone. Candidate plants used for phytostabilization have extensive root systems, are tolerant to Hg toxicity and are adaptive to site-specific environments[251–254]. Phytovolatilization refers to the uptake of elements by plant roots, translocation through the xylem and subsequent emission to the atmosphere[15]. Phytovolatilization is unique to Hg owing to its relatively high volatility; however, there are few studies on phytovolatilization of Hg via vegetation, in part, because of its inefficiency (<0.98% remediation)[255], difficulties in monitoring volatilization fluxes and possibly related to concern over secondary contamination by emitting Hg to the atmosphere.

Instead, most studies on phytoremediation have focused on phytoextraction, whereby Hg is removed from soil by harvesting vegetation that has taken up Hg from soils. No plant has been identified as a Hg hyperaccumulator, which are plants that are capable of growing under high contamination and take up metals via roots and bioconcentrate them in their shoots[256]. Vegetation known to show a potential to bioaccumulate Hg have been shown to remove less than 0.2% of the Hg in Hg-enriched soils, even when chemically assisted[257–260]. Hence, in contrast to some other toxic trace metals where phytoextraction is highly efficient (such as 32.4–84.5% removal of soil cadmium by *Sedum plumbizincicola*)[261], phytoextraction is considered of low efficiency for Hg.

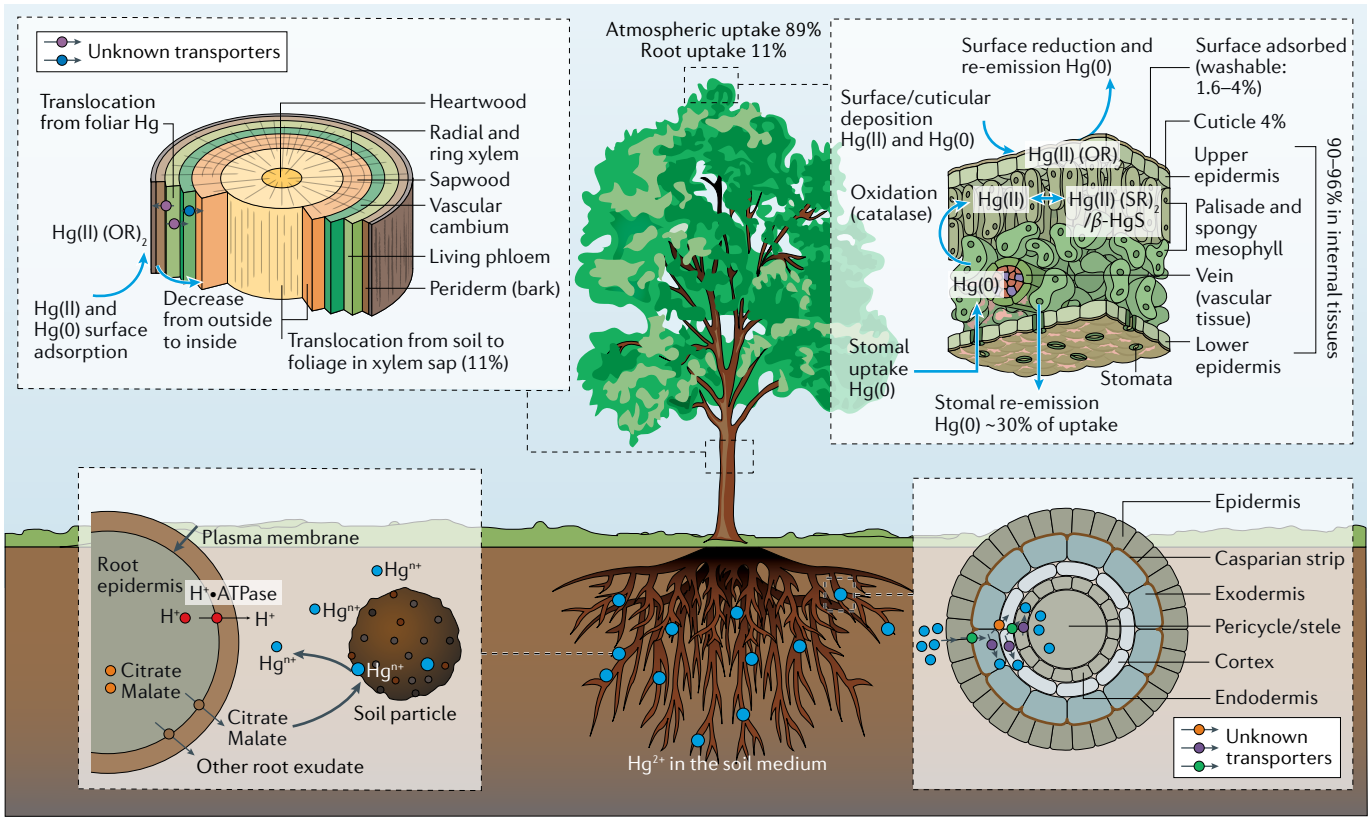

Fig. 2 | **Pathways of plant Hg uptake.** Plants uptake atmospheric mercury (Hg) through their foliage via stomatal and cuticular uptake, and transport Hg through leaf tissues and translocate Hg via phloem transport to woody tissues. Plants also uptake Hg from the soil through their roots, with little transport of Hg through root tissues into xylem. Finally, there is passive uptake of atmospheric Hg to bark. Leaf cross section adapted from REF.[240], Springer Nature Limited.

compared with vascular plants (FIG. 1c; Supplementary Fig. 2). Hg bioaccumulation in mosses and lichens is controlled by numerous biotic and abiotic factors, including: species, whereby different moss and lichen species show large differences in Hg concentrations under the same exposures[113–116]; substrate and local soil[117–119]; growth rate and surface area[120–122]; exposure to pollution source[49]; temporal variation[121]; and chemical composition of wet and dry deposition[123,124]. Metals accumulate in mosses and lichens through intracellular and extracellular processes, as a lack of thick waxy cuticles in lichens and mosses allows cations to diffuse readily through cell walls[125]. In the extracellular process, metals are intercepted and adsorbed and/or absorbed by exchange sites outside of cell walls and plasma membrane surface. In the intracellular process, Hg is subsequently trapped as particles on the cell surface layer or translocated inside the cell[117,126–128]. In addition to surface deposition of oxidized atmospheric Hg (reactive gaseous Hg and particulate-bound Hg), Hg(0) assimilation could contribute to trapping and sequestering Hg in moss and lichen tissue, but the specific methods of uptake, binding and accumulation from the atmosphere are unknown. After uptake, Hg(0) is oxidized to Hg(II) and subsequently immobilized in moss and lichens for 4–5 weeks[49,122,129]. Lichens show significantly higher Hg concentrations (78 $\mu g\,kg^{-1}$ [10–180 $\mu g\,kg^{-1}$]) than mosses (51 $\mu g\,kg^{-1}$ [2–165 $\mu g\,kg^{-1}$]) in our data set ($P<0.05$) (FIG. 1c). This difference is likely related to the different morpho-physiological properties and abilities to intercept airborne particles of lichens and mosses[122], as lichens often accumulate higher contents of atmosphile elements (derived from atmospheric sources), whereas mosses have shown higher contents of lithophile elements, such as dust[130–132].

Staple isotope analyses indicate that atmospheric Hg(0) accounts for 76% and 86% in ground and tree mosses, with the remaining 24% and 14% originating from Hg(II) contribution[111]. Hence, where lichens and mosses represent a significant component of plant communities, such as in the Arctic tundra, their high tissue concentrations are responsible for high atmospheric deposition loads via uptake of atmospheric Hg exceeding Hg deposition by vascular plants[2,58]. Furthermore, Hg concentrations in mosses and lichens can maintain a state of dynamic equilibrium with atmospheric Hg concentrations[133,134], and lichens and mosses increase Hg(0) uptake from the atmosphere when exposure is high[115]. Passive biomonitoring using lichens and mosses for atmospheric Hg could, hence, be cost-effective and benefit from abundant distribution, structural simplicity, rapid growth rate and ease of sampling[125,128,135], but this application has shown limited success. For example, there were weak correlations between atmospheric Hg deposition and Hg accumulation in moss and soils across large south-to-north gradients in Norway[136].

In contrast, there was a lack of correlation between modelled atmospheric Hg deposition and moss concentrations across a large network of sites in Europe, and moss collected in Norway showed no distinct north-to-south patterns, in spite of expected gradients in atmospheric Hg pollution[137]. Therefore, and consistent with previous reviews[122,125], we conclude that Hg concentrations in lichens and mosses are impacted by many environmental variables, which complicates its use as a biomonitor for atmospheric Hg concentrations and deposition.

Vegetation–atmosphere Hg exchange

Foliage and the atmosphere show dynamic and complex exchanges of Hg, including via the following three pathways: bidirectional Hg(0) exchange at the interface of foliage and the atmosphere[43,53,57,80–82,93,138–140]; assimilation of divalent Hg(II) wet and particle deposition (particulate-bound Hg and reactive gaseous Hg) by foliage, followed by partial or full re-emission to the atmosphere as Hg(0) after photochemical reduction[55,60,140]; and transpiration of Hg from soils to foliage, whereby Hg(0) is subsequently emitted, either directly or after photochemical reduction[62,79,86,141,142]. Several studies, however, have shown that soil Hg concentrations generally do not influence leaf–atmosphere exchange fluxes[50,53,138,143,144], supporting the idea that there is limited root-to-atmosphere transport of Hg (such as via transpiration).

Most foliage flux studies show net uptake of Hg(0), providing evidence of foliar sinks of atmospheric Hg(0) (REF.[145]), but bidirectional exchanges of Hg(0) were also observed. For example, foliage was a net sink in broadleaved forest, coniferous forests and a wetland[57,80,93,140], whereas other measurements (such as those taken in a salt marsh and a subtropical coniferous forest) indicated vegetation was net Hg(0) sources to the atmosphere[82,139]. Some variability among studies could be explained by differences in solar radiation, as radiation favours photochemical re-emissions, an observation further supported by diurnal flux variability that shows net emissions during peak solar radiation at midday[57,82]. However, variability in flux directions over foliage could also be attributable to methodological challenges, as these fluxes are small and difficult to measure[146]. Exposures to elevated Hg(0) concentrations generally increase net deposition to leaves[43,53,81], and it has been proposed that foliage–atmosphere fluxes are dependent on atmospheric compensation points[145,147]. Most compensation points are reported to be near or lower than ambient atmospheric Hg concentrations, so that, under non-contaminated conditions, net Hg deposition to foliage should dominate[80,140]. Canopies also shield soil surfaces from incident solar radiation, which strongly reduces underlying soil Hg(0) emission[145,148–150].

Studies of land–atmosphere Hg fluxes at the ecosystem level are used to quantify dry gaseous component of Hg(0) deposition over land. Whole-ecosystem Hg(0) exchange flux studies are largely based on micrometeorological tower techniques and commonly report net Hg(0) deposition during peak vegetation season[2,70,71,80,151–156], supporting net Hg assimilation by vegetation. Although time-extended measurements are rare, a few annual time series exist and show net annual deposition of gaseous Hg(0) between 2 and 29 $\mu g\,m^{-2}$ per year over grassland and tundra ecosystems[21,152,156]. Studies over wetlands, in contrast, report net Hg(0) emissions (9.4–18.4 $\mu g\,m^{-2}$ per year)[69,157], as do forests impacted by regional pollution (58 and 2.6 $\mu g\,m^{-2}$ per year)[158]. The dominance of net Hg(0) deposition measured during peak vegetation in upland, non-polluted ecosystems is also in contrast with studies of agricultural and bare soil surfaces, in which net Hg(0) emissions dominated (55.3 $ng\,m^{-2}\,h^{-1}$ over bare soil, corn and snow-covered fields in Canada[159], and 5.5–10.8 $ng\,m^{-2}\,h^{-1}$ over bare soil, wheat and corn in agricultural fields in China[160]). Notably, though, a review of available terrestrial surface–atmosphere Hg(0) flux studies reveals that, based on the current measurements available, global assimilation by vegetation cannot be determined accurately, as global flux uncertainty over canopies ranges from a net deposition of 513 Mg to a net emission of 1,353 Mg per year[145].

Hg stable isotopes provide a fingerprint of the sources and transformation processes in environmental samples[1,161,162]. The seven stable isotopes of Hg undergo mass-dependent fractionation (δ^{202}Hg) and mass-independent fractionation of odd-mass (odd-MIF, Δ^{199}Hg and Δ^{201}Hg) and even-mass (even-MIF, Δ^{200}Hg and Δ^{204}Hg) numbered isotopes. Even-MIF is thought to be exclusively produced in the upper atmosphere, providing a conservative tracer for atmospheric Hg species deposited to the Earth surface[163]. Atmospheric Hg(0) and Hg(II) in rainfall are characterized by distinct isotope even-MIF signatures (FIG. 3). Specifically, Δ^{200}Hg of Hg(II) in rainfall exhibits positive anomalies of 0.2‰ (0.13‰ to −0.24‰ IQR, $n = 115$) and the corresponding pool of atmospheric Hg(0) slightly negative Δ^{200}Hg values of −0.05‰ (−0.07‰ to −0.03‰ IQR, $n = 117$)[2,21,164–171]. Δ^{200}Hg measured in foliage of −0.02‰ (−0.05‰ to 0.00‰ IQR, $n = 120$) is similar to the Δ^{200}Hg of atmospheric Hg(0) (REFS[2,167,171–175]), and a mass balance calculation based on Δ^{200}Hg reveals that 88% (79–100% IQR) of Hg in vegetation originates from the uptake of atmospheric Hg(0).

Foliar uptake of Hg(0) discriminates against heavier Hg isotopes (straight arrow in FIG. 3), resulting in the negative δ^{202}Hg values (−1% to −3% relative to atmospheric Hg(0))[2,58,155,163,167,171] typically observed in foliage[2,58,167,171–176], depending on the plant species[58] and proximity to anthropogenic Hg emission sources[171]. Indeed, foliar uptake fractionation factors of −2.6‰[163] and −4.2‰[21] have been reported based on δ^{202}Hg depletion of atmospheric Hg(0). As a result of plant uptake of lighter Hg(0), corresponding enrichments of heavier Hg(0) isotopes in the residual atmospheric Hg(0) pool of the boundary layer has been observed above a high-altitude peat bog in Europe[163], an Arctic tundra[21] and deciduous and evergreen forests in Southeast Asia[71], as indicated by higher δ^{202}Hg values (light red circles in FIG. 3). Vegetation activity, with foliar uptake resulting in higher residual δ^{202}Hg values, and anthropogenic emissions have been identified as the two main drivers for spatial and temporal variation of atmospheric Hg(0) isotope compositions in the Northern Hemisphere[177].

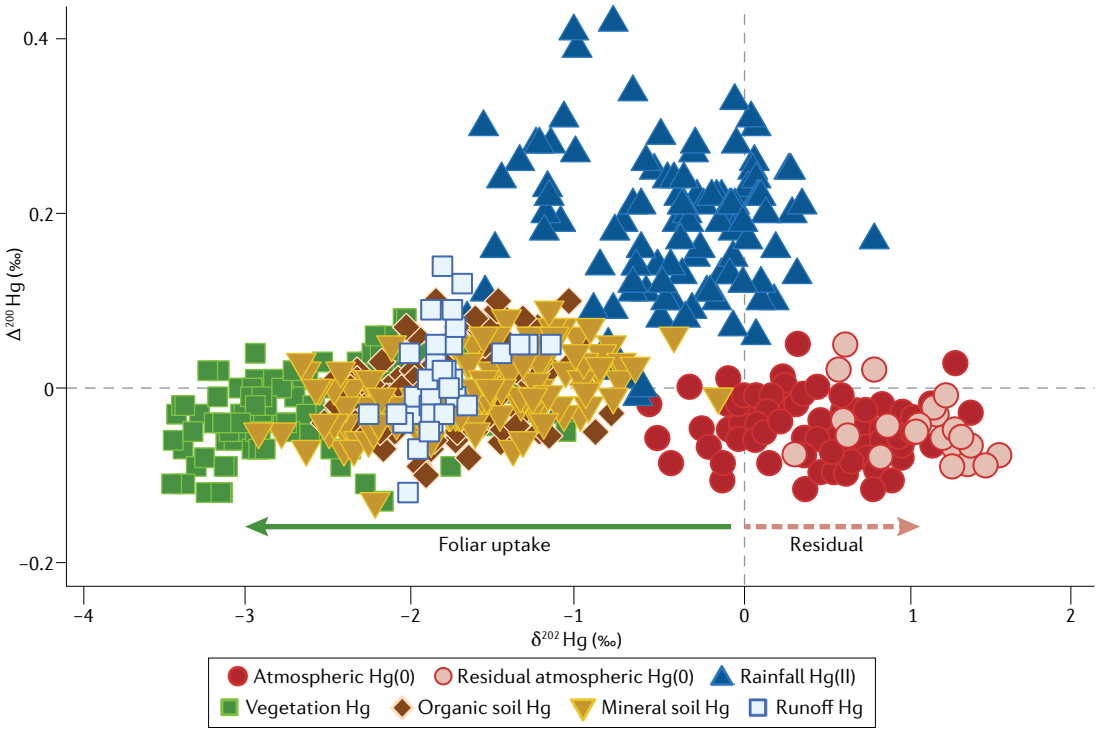

Fig. 3 | **Hg stable isotopes in foliage.** Composition of atmospheric gaseous elemental mercury (Hg(0)) and divalent mercury (Hg(II)) sources, and sources of mercury (Hg) in vegetation and in terrestrial sinks (organic and mineral soils and runoff), plotted as even-mass-independent (Δ^{200}Hg) versus mass-dependent (δ^{202}Hg) isotopes. The solid green arrow represents the Hg isotope fractionation during uptake of Hg(0) by foliage and the light red dashed arrow represents the fractionation of residual Hg(0) in the atmosphere. The figure includes all currently available, peer-reviewed isotope data on vegetation Hg.

A global Hg isotope box model based on δ^{202}Hg and Δ^{200}Hg constraints[178] also supports the findings that terrestrial dry Hg(0) deposition is a critical global flux, supporting a vegetation control on seasonal variation of atmospheric Hg(0) concentrations[23] and in support of vegetation acting as a critical sink for atmospheric Hg(0).

Re-emissions of Hg(0) from foliage from an evergreen forest was associated with odd-MIF, suggesting that Hg incorporated in the leaf structure is photochemically reduced and results in a bidirectional flux of Hg(0) across stomata[155]. Similarly, small depletions in odd-MIF Δ^{199}Hg of approximately −0.1 ‰ in surface soils have been attributed to small losses by photochemical reduction in foliage and litterfall[163,167]. Overall, odd-MIF values show small but consistent re-emission signatures on foliar Hg (Supplementary Fig. 4), providing a promising tool for quantitative assessments of deposition and losses at the ecosystem scale in the future.

Deposition of atmospheric Hg(0) by means of litterfall constitutes the major source of Hg in plants, organic and mineral soils, and watershed runoff (FIG. 3). Average source contributions of atmospheric Hg(0) deposition to soils was 57–94% in North America[167,175], 70% to Arctic tundra soils in Alaska in the USA[2], 79% to a high-altitude peatland in the Pyrenees in France, 90% to boreal forest soils in Sweden[174] and 26% in surface soils of Tibetan wetlands in China[179]. Notably, the estimate in Arctic tundra soils derived by stable Hg isotopes was almost identical to the contribution of Hg(0) to total deposition (71%) based on exchange and deposition measurements[2]. Global-scale mass balance estimations, based on Δ^{200}Hg patterns, reveal contributions of atmospheric Hg(0)-derived Hg of 62% (53–89% IQR) in organic soils[2,167,174–176,180,181] and 84 % (70–92% IQR) in mineral soils (albeit when neglecting geogenic Hg sources)[2,167,173–176,180,181]. Similarly, in runoff of terrestrial ecosystems, 76% (60–92% IQR) of Hg is derived from deposition of atmospheric Hg(0) (REFS[36,176]). The major role and isotope fractionation of foliar uptake of atmospheric Hg(0) results in a characteristic terrestrial fingerprint, which is propagated to and found to be dominant in freshwater and coastal sediments and biota[39,163,182–186].

Global impact of vegetation Hg uptake

Empirical evidence and model results strongly suggest that the dominant pathway of atmospheric Hg deposition in terrestrial ecosystems is dry Hg(0) deposition via vegetation uptake[2,175,187–191]. Moreover, the primary driver of Hg accumulation and storage in surface soils is vegetation uptake of atmospheric Hg(0) (REFS[26,179]). In turn, plant Hg(0) uptake controls seasonal variations and global distribution of atmospheric Hg concentrations[23]. Climate-change-induced alterations in vegetation and human-induced land use changes have substantial impacts on global Hg cycling[1,179]. Here, we review studies on the global impacts of vegetation Hg assimilation on environmental and ecosystem processes based on published empirical studies and modelling results.

Empirical studies. Global estimates of Hg uptake by vegetation are available based on field-based litterfall and throughfall measurements. These studies show that forests are strong sinks of atmospheric Hg(0) (REFS[19,25,26,77,192]), mainly driven by litterfall, which exceeds all other pathways of Hg inputs. Global Hg litterfall fluxes are estimated between 1,180 ± 710 Mg per year and 1,232 Mg per year — approximately cycling one-quarter of the total global atmospheric Hg pool each year (~4,400–5,300 Mg) — based on measurement from over 90 forest sites[187–190]. Litterfall deposition has been proposed to decrease along with primary productivity from tropical to temperate to boreal regions, with approximately 70% of global litterfall deposition estimated to occur in tropical and subtropical regions[190]. However, estimated annual mean Hg(0) dry deposition in terrestrial ecosystems could be enhanced by up to 20% in the northern mid-latitudes by 2050, owing to increases in plant productivity associated with CO_2 fertilization[193]. Throughfall Hg deposition might be of similar magnitude as litterfall deposition and, although much more uncertain than the litterfall estimates, could globally account for 1,340 Mg per year[179], contributing additional Hg deposition in the range of 90%, 75% and 143% of litterfall Hg deposition in China, Europe and North America, respectively[77].

The sum of litterfall plus throughfall deposition represents a lower-bound estimate of total vegetation Hg uptake because it does not account for Hg deposition via woody tissues, non-vascular lichen and mosses, and whole-plant die-off (such as tree blowdown), nor does it account for direct soil uptake[1]. For example, studies report that Hg mass in tree wood is severalfold higher than the Hg mass contained in canopies[194–197], and woody tissues (tree turnover) could account for 60% of litterfall deposition[198], in spite of relatively slow wood turnover rates. Indeed, analysis along a forest succession suggests that combined woody biomass, moss and throughfall deposition exceeds that of litterfall, thus, using litterfall deposition only would strongly underestimate Hg accumulation in forest soils[179]. If substantial amounts of root Hg are, indeed, also derived from atmospheric uptake[111], root turnover will further increase atmospheric dry deposition. After plant-bound Hg is transferred to soils and forest floors, the fate and mobility of Hg in soils and watersheds depends on litter decomposition and biogeochemical cycling of organic matter[91,199–203]. During litter decomposition, the total mass and concentrations of Hg increase, owing to relatively stronger losses of carbon compared with Hg and to continued absorption of Hg from precipitation and throughfall during the initial stages of litter decomposition[199,202,204]. Stable Hg isotope studies suggest that microbial reduction and photoreduction also play a role in Hg losses from litter and soils[174,203], possibly leading to large re-evasion losses over long time periods. Still, large amounts of plant-derived Hg are likely retained in soils, leading to large pools of soil Hg globally[1,179,205].

Vegetation Hg uptake in models. In addition to empirical measurements, global models are used to investigate terrestrial–atmosphere Hg exchange processes[146,188,206,207]. The dry deposition of Hg, driven by advection–diffusion in air and heterogeneous uptake by surfaces[208], is generally parameterized in models using an inferential approach (in other words, as the product of ambient Hg concentration and modelled dry deposition velocity)[10,209–213]. Dry deposition velocities over vegetation canopies are estimated through a resistance analogy that includes aerodynamic, soil, stomatal and cuticle resistances[214–217]. Parameters for oxidized Hg(II) species deposition are selected based on similarity of solubility and reactivity of Hg with other well-studied atmospheric compounds[218]. A wide range of Hg(0) dry deposition schemes have been implemented in models; early studies assumed small and constant deposition velocities over vegetated surfaces or neglected Hg(0) deposition altogether, whereas resistance-based Hg(0) deposition schemes are commonly employed now[219]. Terrestrial Hg(0) emissions are parameterized as a function of environmental conditions (including temperature, solar irradiance and leaf area index) and soil Hg content, and often include a fraction of recently deposited Hg to soils, vegetation and snow as prompt re-emissions[220–228].

A few bidirectional air–surface Hg exchange schemes have been developed and implemented in regional models[206,220,229,230]. For example, Hg exchange fluxes over canopies have been formulated as concentration gradients across air–foliage by defining dynamic compensation points based on partitioning coefficients[229]. This model was subsequently revised[230] by updating surface resistances[216,217,231] and implementing photochemical reduction of Hg in foliage[232]. In another example, Hg(0) compensation points over a variety of canopies and environmental conditions in North America were reviewed (range 0.5–33 ng m^{-3})[206], and a bidirectional air–surface exchange model based on a dry deposition scheme[216,217] and empirical compensation points was developed. However, dry deposition parameterization is highly sensitive to resistance parameters, some of which are poorly constrained for Hg (REFS[61,233]). In addition, bidirectional Hg exchange schemes depend on numerous ill-constrained parameters and oversimplified chemistry[206,229,230]. Based on direct micrometeorological measurements of Hg(0) fluxes, it has been recommended that current models should increase stomatal resistances to reduce overestimation of stomatal uptake of Hg(0) (for example, by a factor of 5–7) and simultaneously increase ground and cuticular uptake to mimic night-time and wintertime Hg(0) deposition (by factors of 3–4 and 2–4, respectively)[234]. In general, there is a need for mechanistic bidirectional air–foliage Hg partitioning schemes that incorporate biome-specific biomass data, plant physiology, redox chemistry and environmental variables (temperature, light, moisture, atmospheric turbulence)[146,207].

Model simulations. We performed two global model simulations using the GEM-MACH-Hg model[191,219,221,235–237] to assess the impacts of vegetation Hg uptake on contemporary atmospheric Hg cycling (year 2015); one with and a second without the presence of vegetation (see details of the modelling approach in the Supplementary Information). The simulation without vegetation cover

Physiology
The study of plant function and behaviour, including growth, metabolism, reproduction, defence and communication.

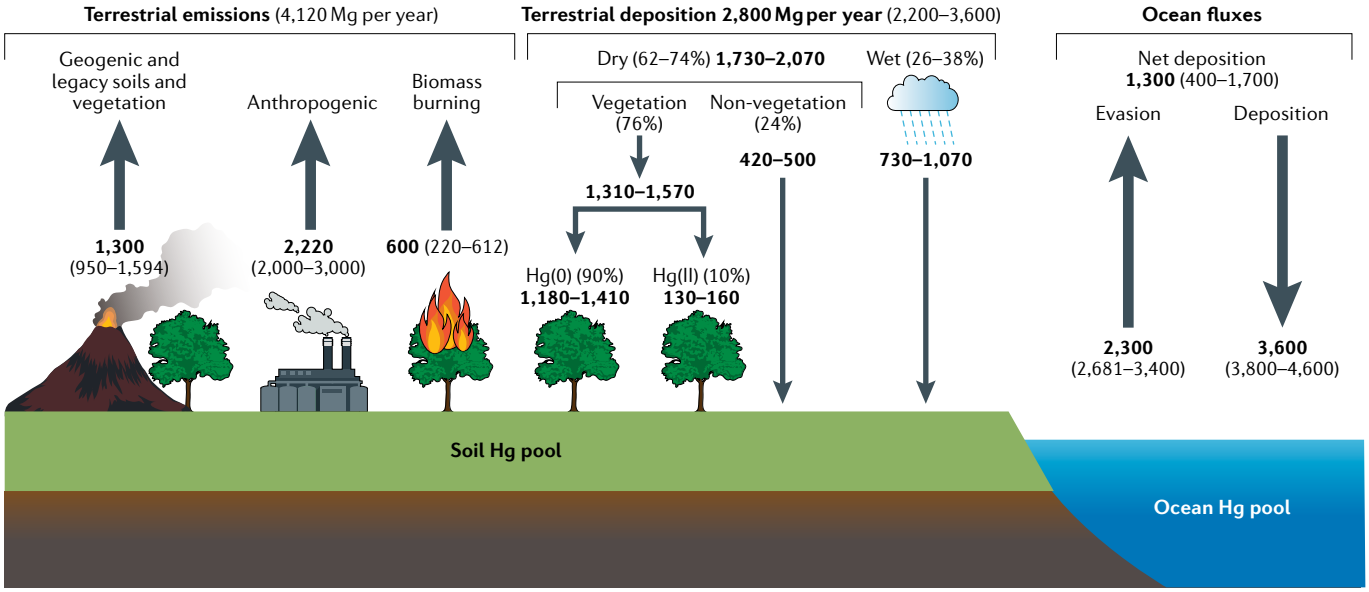

Fig. 4 | **Global Hg cycle.** Mercury (Hg) emissions include natural, anthropogenic and legacy sources. Terrestrial deposition includes dry (62–74% of terrestrial deposition) and wet (26–38%) deposition, where dry deposition is separated further into vegetation Hg uptake (gaseous elemental mercury (Hg(0)) and divalent mercury (Hg(II))), which accounts for 76% of terrestrial uptake, and deposition to non-vegetation surfaces (soils, snow and water; 24% of uptake) using GEM-MACH-Hg model simulations (this Review). GEM-MACH-Hg model estimates are in bold and peer-reviewed literature ranges are in parentheses. Origins of literature fluxes are given in Supplementary Table 1. The units for the emission and deposition are in Mg Hg per year.

was configured by replacing all biome types to desert, while keeping primary (geogenic and anthropogenic) and secondary (recycling of historic deposition) Hg emissions unchanged. These simulations allowed examination of the impact of vegetation Hg uptake on the residence time of Hg in the atmosphere and spatiotemporal distribution of Hg in air and Hg deposition to the Earth's ecosystems (FIG. 4; Supplementary Table 1).

GEM-MACH-Hg simulations here estimate global annual total Hg deposition of approximately 6,400 Mg, with about 44% deposited to terrestrial ecosystems (~2,800 Mg per year, in line with the literature range of 2,200–3,600 Mg per year)[6,8,9]. Global terrestrial wet deposition is estimated to be in the range of 730–1,070 Mg per year, accounting for only 26–38% of total terrestrial deposition. Estimated dry Hg deposition (combined surface uptake and particulate gravitational settling)[217] dominates across terrestrial environments and is in the range of 1,730–2,070 Mg per year (62–74% of terrestrial deposition). Direct vegetation uptake accounts for the largest portion of this deposition (1,310–1,570 Mg per year). Hg(0) accounts for approximately 90% of foliage Hg uptake and represents the single largest terrestrial removal pathway of atmospheric Hg (1,180–1,410 Mg per year). Global oceans are a net sink for atmospheric Hg, with annual net deposition (deposition minus emission) reported in the literature ranging from 400 to 1,700 Mg per year[6,8,9], and a GEM-MACH-Hg model estimate here of 1,300 Mg per year.

Comparison of GEM-MACH-Hg simulations with and without vegetation show that Hg uptake by vegetation reduces the residence time of atmospheric Hg(0) from 10 to 8 months (thus, reduces global atmospheric Hg(0) concentrations) (FIG. 5a,b) and lessens the global atmospheric Hg(0) burden from 5,120 to 4,460 Mg. The vegetation Hg sink notably reduces air concentrations of Hg(0) over forested regions, by 25% over eastern North America and by 35% over boreal forests in Europe, for example (FIG. 5a,b). Uptake of Hg transported out of the source regions by local and regional vegetation lowers the long-range transport and deposition of Hg in remote regions such as the Arctic and global oceans (FIG. 5c,d). In the absence of vegetation cover, the majority of emitted Hg would be removed from the atmosphere by wet deposition (over land and oceans), thereby, repartitioning the deposition between land (29%) and ocean (71%), and increasing the Hg deposition to global oceans by approximately 960 Mg per year (FIG. 5d).

Vegetation Hg uptake reduces the inter-hemispheric gradient (Northern Hemisphere versus Southern Hemisphere) of Hg(0) from 1.8:1.1 ng m^{-3} to 1.5:1.0 ng m^{-3} (FIG. 6a). Seasonal atmospheric Hg(0) concentrations are characterized by winter to early spring maxima and late summer to fall minima, especially over vegetated surfaces in the Northern Hemisphere (FIG. 6b and Supplementary Figs 5–8). In contrast, Southern Hemispheric locations lack systematic seasonal cycles (FIG. 6c; Supplementary Fig. 9). Our model analyses suggest that Northern Hemispheric seasonal Hg(0) cycles over land are controlled by (in order of importance): vegetation uptake (summer and fall maximum); terrestrial soil and vegetation emissions (summer maximum); cryosphere re-emissions (spring peak and fall minimum); and wildfire emissions (spring to summer). Continued deposition of Hg(0) to the biosphere into the fall results in hemispheric-scale depletion of ambient Hg(0) concentrations in late summer to fall months.

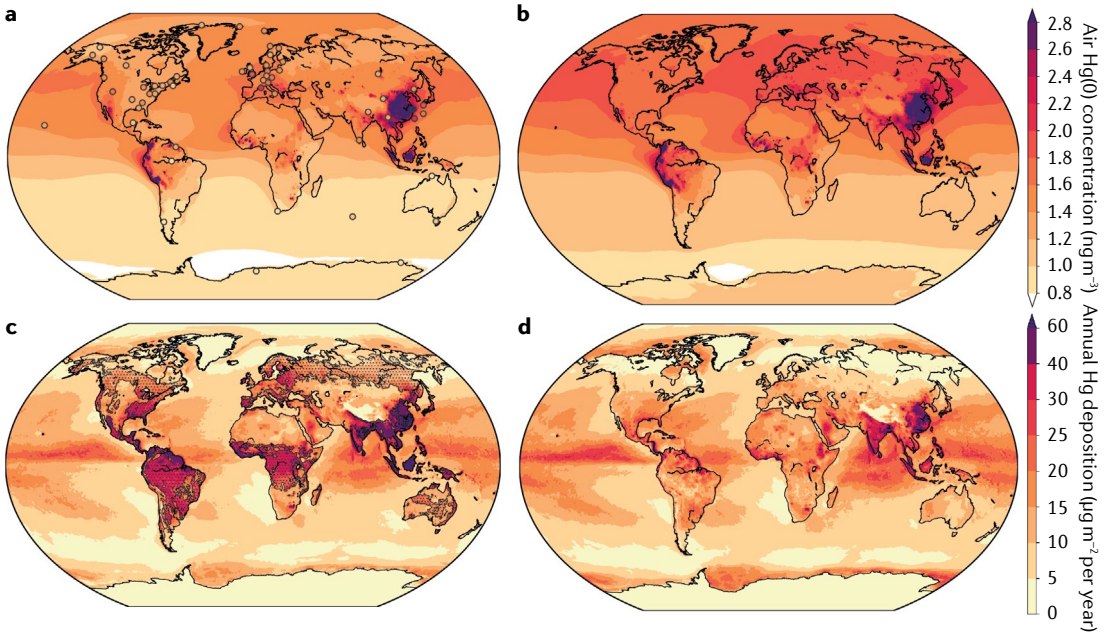

Fig. 5 | **Global surface air concentrations and annual deposition of Hg. a** | Global annual average surface air gaseous elemental mercury (Hg(0)) concentrations simulated by the GEM-MACH-Hg model for the year 2015 with vegetation cover present. Available observations of Hg(0) concentrations are indicated in circles; nearby sites are combined and replaced with median values. **b** | Simulation with vegetation cover absent. **c** | Simulated annual mercury (Hg) deposition (total wet and dry deposition) for the year 2015 with vegetation cover present (hatched areas indicate regions of forested vegetation). **d** | Simulated annual Hg deposition with vegetation cover absent. Observations from: CAPMoN, ECCC[241]; AMNet[242]; EMEP[243]; GMOS[244]; Mace Head[245]; Cape Point and Amsterdam Island[246]; Cape Grim[247]; Gunn Point[248]; Mount Lulin[249].

In the absence of Hg uptake by vegetation, atmospheric Hg(0) concentrations increase and pronounced seasonal variations are lost (yellow lines, FIG. 6b and Supplementary Figs 4–7). In the Southern Hemisphere, more variable and less distinct seasonal cycles of Hg(0) are reported (FIG. 6c; Supplementary Fig. 9). These model results are consistent with a previous global analysis of atmospheric data that concluded that seasonality in Hg(0) was strongly related to leaf area cover, and that summertime minima at remote sites in the Northern Hemisphere were best explained by seasonal vegetation uptake[22].

Global Hg deposition is largest in areas of high atmospheric Hg concentrations associated with anthropogenic emission regions (such as Southeast Asia) and areas of high biomass production (such as the Amazon region and the Congo Basin) (FIG. 5c). GEM-MACH-Hg estimates of annual (median) dry deposition Hg fluxes to major global biomes are as follows (see comparison with litterfall-inferred values in Supplementary Table 2)[190]: tropical moist broadleaf forests: 27.3 μg m^{-2} per year; tropical dry broadleaf forests: 24.6 μg m^{-2} per year; temperate broadleaf/mixed forests: 18.3 μg m^{-2} per year; tropical grasslands: 16.4 μg m^{-2} per year, temperate conifers: 14.3 μg m^{-2} per year; temperate grasslands: 9.2 μg m^{-2} per year; boreal forests: 8.3 μg m^{-2} per year; and Arctic tundra: 4.2 μg m^{-2} per year. Underestimation of model deposition to vegetation in tropical forests might be linked to the adsorption of wet deposition on foliage[55,140], as partitioning of Hg wet deposition between foliage and ground is currently not represented in models.

Moreover, there are uncertainties in the analyses here related to the representation of redox processes and heterogeneous Hg chemistry in terrestrial components such as vegetation, soils and snow (reflected in the estimated range of fluxes), as well as legacy Hg cycling in soils (such as from past deposition), which was not examined. Overall, the impacts of vegetation on legacy Hg fluxes are complex and require further knowledge of terrestrial Hg accumulation, speciation and lifetime for formulations in three-dimensional atmosphere–land–ocean biogeochemical models[238,239] (Supplementary Information).

Summary and future perspectives

Vegetation uptake of atmospheric Hg is the most important Hg deposition pathway to the terrestrial environment. Studies based on Hg stable isotopes, enriched isotope tracer experiments, laboratory and ecosystem-level flux measurements, and model simulations consistently show that approximately 90% of Hg in foliage originates from the uptake of atmospheric Hg(0). Ultimately, atmospheric Hg taken up by vegetation and deposited to soils is transferred to downstream aquatic freshwater ecosystems and coastal seas, representing a major source of Hg for aquatic organisms.

A number of areas require further research in order to improve our understanding of the processes controlling Hg uptake by vegetation and its implications to global Hg cycling. In particular, assessment of the impact of climate and land use changes on global Hg cycling are currently hampered by a series of shortcomings in process understanding, observational constraints and

model representations. For example, important knowledge gaps exist with respect to the vegetation interfacial Hg exchange processes; a mechanistic and quantitative knowledge of heterogeneous biochemical processes of plant tissue and soil Hg uptake, considering physiological and environmental drivers, is needed. Progress in these fields could be reached via extended use and interpretations of stable Hg isotopes, molecular and cellular-level tracing experiments to determine transport and biochemical behaviour of Hg in plant cells and tissues, high-resolution mapping of Hg distribution within plant tissues and improved chemical speciation of Hg in plants, such as using synchrotron-based X-ray absorption spectroscopy techniques.

In order to allow better comparison of data, future field studies on Hg in vegetation should report detailed descriptions of the sampling, such as locations within the canopy, time of sampling and needle age in coniferous trees, and, ideally, follow standardized sampling protocols and report environmental exposures (atmosphere and soils). We call for the integration of Hg data in litterfall and throughfall deposition monitoring networks across all biomes, with a particular focus given to areas of high net primary production, such as tropical forests and biomes, where, currently, observational data are scarce, such as grasslands.

Although frequently taken, litterfall and throughfall measurements alone are not sufficient to estimate

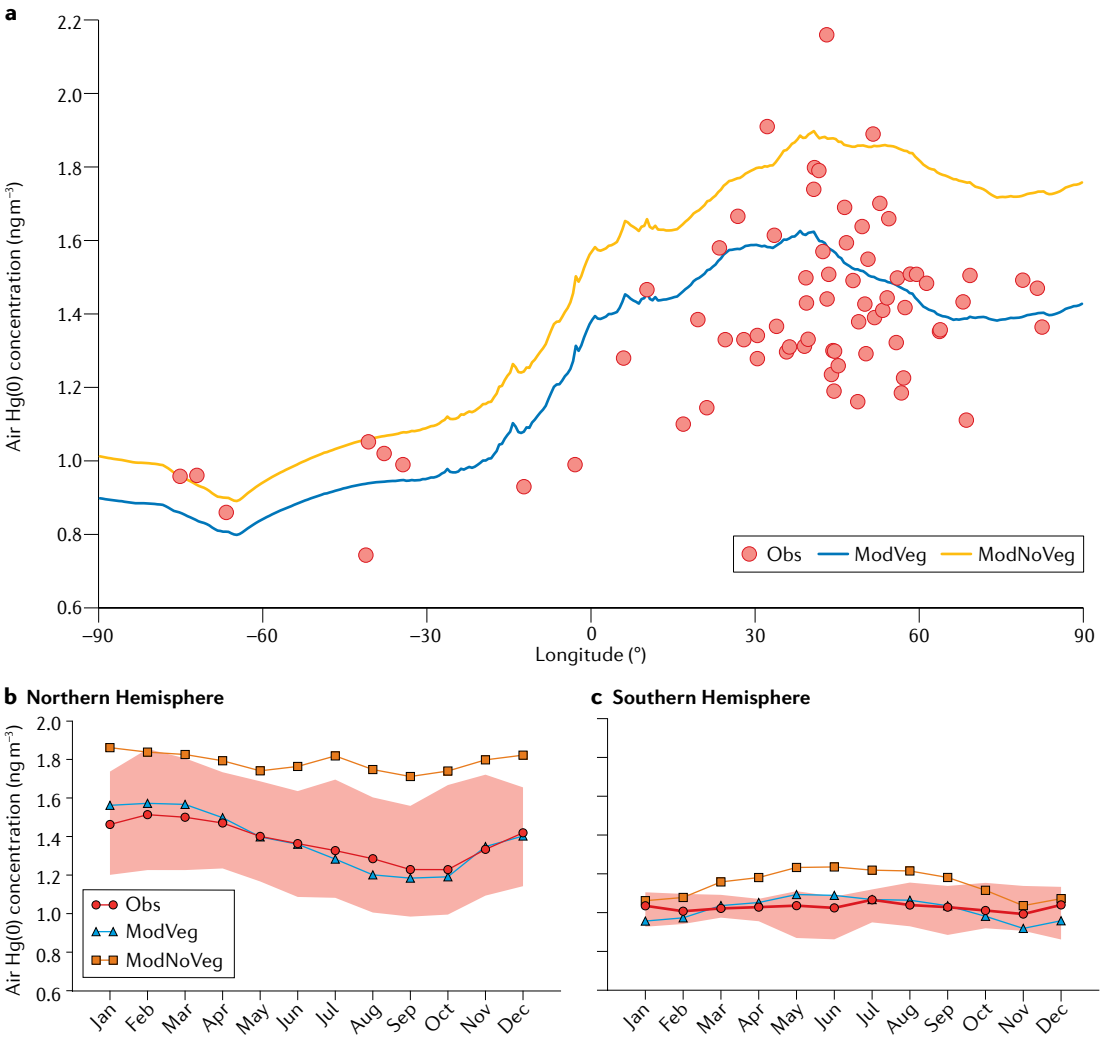

Fig. 6 | **Surface air Hg(0) concentrations. a** | Average surface air gaseous elemental mercury (Hg(0)) concentrations, along with the global hemispheric gradient, simulated by GEM-MACH-Hg for 2015 with and without vegetation cover present. Blue line represents model simulation with vegetation present, yellow line represents model simulation without vegetation present and red dots represent measurement observations. Model simulated lines represent averaged Hg(0) concentrations in 0.5° latitude bands including oceanic regions; observations represent sites mostly located over land and in North America and Europe. **b** | Average measured and simulated (by the GEM-MACH-Hg model at the observation sites) seasonal cycles of surface air Hg(0) concentrations in the Northern Hemisphere; coastal and urban sites were excluding from averaging in the Northern Hemisphere. Blue and yellow lines represent model simulations with vegetation present and without vegetation present, respectively, for 2015. Red line and shaded area represent median of available measurements between 2009 and 2018 and 5th–95th percentiles, respectively. **c** | Seasonal surface air Hg(0) concentrations in the Southern Hemisphere. Seasonal cycle is the average of two sites, Cape Point and Amsterdam Island.

whole-ecosystem Hg deposition, as they do not account for the deposition by woody tissues, translocation to roots, uptake by cryptogamic vegetation and direct sorption of Hg(0) to soils and forest floors. Hence, we recommend measurements of annual time series of ecosystem-level Hg(0) deposition across all major representative global biomes to constrain their net sinks. Furthermore, substantial uncertainties exist in the model parameterizations of surface uptake processes of Hg species, preventing accurate determination of the relative roles of wet and dry deposition and elemental and oxidized Hg species in atmosphere–terrestrial Hg exchange processes.

Finally, amounts and geospatial distribution of soil Hg and secondary Hg emissions (legacy soil and wildfire emissions) are profoundly impacted by foliage Hg uptake, and changes in vegetation cover would alter these. Dynamically coupled Hg models of atmosphere, terrestrial and ocean environments are needed to simulate the effects of both direct and indirect changes in vegetation; measurement and modelling innovations providing mechanistic knowledge of Hg processes in terrestrial ecosystems is critical to achieving this goal.

Published online: 16 March 2021

1. Obrist, D. et al. A review of global environmental mercury processes in response to human and natural perturbations: Changes of emissions, climate, and land use. *Ambio* **47**, 116–140 (2018). **Reviews Hg wet and dry deposition to terrestrial ecosystems, ocean Hg(0) evasion to the atmosphere, global aquatic Hg releases and predicts that land use and climate change impacts on Hg cycling will be large**.
2. Obrist, D. et al. Tundra uptake of atmospheric elemental mercury drives Arctic mercury pollution. *Nature* **547**, 201–204 (2017). **Finds 71% of total Hg deposition over 2 years was derived from gaseous dry deposition of Hg(0), consistent with source characterization in plants and soils using stable Hg isotopes**.
3. Mao, H., Cheng, I. & Zhang, L. Current understanding of the driving mechanisms for spatiotemporal variations of atmospheric speciated mercury: a review. *Atmos. Chem. Phys.* **16**, 12897–12924 (2016).
4. Selin, H. et al. Linking science and policy to support the implementation of the Minamata Convention on Mercury. *Ambio* **47**, 198–215 (2018).
5. United Nations Environment Programme. UNEP chemicals and health branch. *Geneva Environment Network* https://www.genevaenvironmentnetwork.org/environment-geneva/organizations/unep-chemicals-and-waste-branch/ (2019).
6. Horowitz, H. M. et al. A new mechanism for atmospheric mercury redox chemistry: implications for the global mercury budget. *Atmos. Chem. Phys.* **17**, 6353–6371 (2017).
7. Kumar, A., Wu, S., Huang, Y., Liao, H. & Kaplan, J. O. Mercury from wildfires: Global emission inventories and sensitivity to 2000–2050 global change. *Atmos. Environ.* **173**, 6–15 (2018).
8. Outridge, P. M., Mason, R. P., Wang, F., Guerrero, S. & Heimburger-Boavida, L. E. Updated global and oceanic mercury budgets for the United Nations Global Mercury Assessment 2018. *Environ. Sci. Technol.* **52**, 11466–11477 (2018). **Presents a current understanding of the global environmental Hg cycling by reporting estimates and uncertainties of global Hg emissions, fluxes and budgets**.
9. Cohen, M. D. et al. Modeling the global atmospheric transport and deposition of mercury to the Great Lakes. *Elementa Sci. Anthrop.* **4**, 000118 (2016).
10. Song, S. et al. Top-down constraints on atmospheric mercury emissions and implications for global biogeochemical cycling. *Atmos. Chem. Phys.* **15**, 7103–7125 (2015).
11. Zhang, Y. et al. A coupled global atmosphere-ocean model for air-sea exchange of mercury: Insights into wet deposition and atmospheric redox chemistry. *Environ. Sci. Technol.* **53**, 5052–5061 (2019).
12. Iverfeldt, Å. Mercury in forest canopy throughfall water and its relation to atmospheric deposition. *Water Air Soil Pollut.* **56**, 553–564 (1991).
13. Munthe, J., Hultberg, H. & Iverfeldt, A. Mechanisms of deposition of methylmercury and mercury to coniferous forests. *Water Air Soil Pollut.* **80**, 363–371 (1995).
14. Niu, Z. C., Zhang, X. S., Wang, Z. W. & Ci, Z. J. Field controlled experiments of mercury accumulation in crops from air and soil. *Environ. Pollut.* **159**, 2684–2689 (2011).
15. Wang, J., Feng, X., Anderson, C. W., Xing, Y. & Shang, L. Remediation of mercury contaminated sites–a review. *J. Hazard. Mater.* **221-222**, 1–18 (2012).
16. Ranieri, E. et al. Phytoextraction technologies for mercury- and chromium-contaminated soil: a review. *J. Chem. Technol. Biotechnol.* **95**, 317–327 (2020).
17. Hou, D. et al. Metal contamination and bioremediation of agricultural soils for food safety and sustainability. *Nat. Rev. Earth Environ.* **1**, 366–381 (2020).
18. Grigal, D., Kolka, R., Fleck, J. & Nater, E. Mercury budget of an upland-peatland watershed. *Biogeochemistry* **50**, 95–109 (2000).
19. Grigal, D. F. Mercury sequestration in forests and peatlands: A review. *J. Environ. Qual.* **32**, 393–405 (2003).
20. St. Louis, V. et al. Importance of the forest canopy to fluxes of methyl mercury and total mercury to boreal ecosystems. *Environ. Sci. Technol.* **35**, 3089–3098 (2001).
21. Jiskra, M., Sonke, J. E., Agnan, Y., Helmig, D. & Obrist, D. Insights from mercury stable isotopes on terrestrial–atmosphere exchange of Hg(0) in the Arctic tundra. *Biogeosciences* **16**, 4051–4064 (2019).
22. Uprety, S. & Cao, C. Radiometric comparison of 1.6-μm CO_2 absorption band of Greenhouse Gases Observing Satellite (GOSAT) TANSO-FTS with Suomi-NPP VIIRS SWIR band. *J. Atmos. Ocean Technol.* **33**, 1443–1453 (2016).
23. Jiskra, M. et al. A vegetation control on seasonal variations in global atmospheric mercury concentrations. *Nat. Geosci.* **11**, 244–250 (2018). **Shows terrestrial vegetation acts as a global Hg(0) pump, which controls seasonal variations of atmospheric Hg(0)**.
24. Obrist, D. et al. A synthesis of terrestrial mercury in the western United States: Spatial distribution defined by land cover and plant productivity. *Sci. Total Environ.* **568**, 522–535 (2016).
25. Obrist, D. Mercury distribution across 14 U.S. forests. Part II: Patterns of methyl mercury concentrations and areal mass of total and methyl mercury. *Environ. Sci. Technol.* **46**, 5921–5930 (2012).
26. Obrist, D. et al. Mercury distribution across 14 U.S. forests. Part I: Spatial patterns of concentrations in biomass, litter, and soils. *Environ. Sci. Technol.* **45**, 3974–3981 (2011).
27. Evers, D. C. et al. Biological mercury hotspots in the northeastern United States and southeastern Canada. *Bioscience* **57**, 29–43 (2007).
28. Driscoll, C. T. et al. Mercury contamination in forest and freshwater ecosystems in the northeastern United States. *Bioscience* **57**, 17–28 (2007).
29. Fleck, J. A. et al. Mercury and methylmercury in aquatic sediment across western North America. *Sci. Total. Environ.* **568**, 727–738 (2016).
30. Hsu-Kim, H. et al. Challenges and opportunities for managing aquatic mercury pollution in altered landscapes. *Ambio* **47**, 141–169 (2018).
31. Shanley, J. B. et al. Comparison of total mercury and methylmercury cycling at five sites using the small watershed approach. *Environ. Pollut.* **154**, 143–154 (2008).
32. Riscassi, A. L. & Scanlon, T. M. Particulate and dissolved mercury export in streamwater within three mid-Appalachian forested watersheds in the US. *J. Hydrol.* **501**, 92–100 (2013).
33. Sonke, J. E. et al. Eurasian river spring flood observations support net Arctic Ocean mercury export to the atmosphere and Atlantic Ocean. *Proc. Natl Acad. Sci. USA* **115**, E11586–E11594 (2018).
34. Douglas, T. A. & Blum, J. D. Mercury isotopes reveal atmospheric gaseous mercury deposition directly to the Arctic coastal snowpack. *Environ. Sci. Technol. Lett.* **6**, 235–242 (2019).
35. Strok, M., Baya, P. A., Dietrich, D., Dimock, B. & Hintelmann, H. Mercury speciation and mercury stable isotope composition in sediments from the Canadian Arctic Archipelago. *Sci. Total. Environ.* **671**, 655–665 (2019).
36. Jiskra, M., Wiederhold, J. G., Skyllberg, U., Kronberg, R.-M. & Kretzschmar, R. Source tracing of natural organic matter bound mercury in boreal forest runoff with mercury stable isotopes. *Environ. Sci. Process. Impacts* **19**, 1235–1248 (2017).
37. Janssen, S. et al. Chemical and physical controls on mercury source signatures in stream fish from the northeastern United States. *Environ. Sci. Technol.* **53**, 10110–10119 (2019).
38. Madigan, D. et al. Mercury stable isotopes reveal influence of foraging depth on mercury concentrations and growth in Pacific bluefin tuna. *Environ. Sci. Technol.* **52**, 6256–6264 (2018).
39. Li, M. et al. Environmental origins of methylmercury accumulated in subarctic estuarine fish indicated by mercury stable isotopes. *Environ. Sci. Technol.* **50**, 11559–11568 (2016).
40. Arnold, J., Gustin, M. S. & Weisberg, P. J. Evidence for nonstomatal uptake of Hg by aspen and translocation of Hg from foliage to tree rings in Austrian pine. *Environ. Sci. Technol.* **52**, 1174–1182 (2018). **Reveals Hg accumulation into tree rings via stomata and subsequent translocation by way of phloem, and highlights that the use of trees as temporal proxies requires further investigation**.
41. Peckham, M. A., Gustin, M. S., Weisberg, P. J. & Weiss-Penzias, P. Results of a controlled field experiment to assess the use of tree tissue concentrations as bioindicators of air Hg. *Biogeochemistry* **142**, 265–279 (2019).
42. Greger, M., Wang, Y. D. & Neuschutz, C. Absence of Hg transpiration by shoot after Hg uptake by roots of six terrestrial plant species. *Environ. Pollut.* **134**, 201–208 (2005).
43. Stamenkovic, J. & Gustin, M. S. Nonstomatal versus stomatal uptake of atmospheric mercury. *Environ. Sci. Technol.* **43**, 1367–1372 (2009).
44. Chiarantini, L. et al. Black pine (*Pinus nigra*) barks as biomonitors of airborne mercury pollution. *Sci. Total. Environ.* **569**, 105–113 (2016).
45. Cocking, D., Rohrer, M., Thomas, R., Walker, J. & Ward, D. Effects of root morphology and Hg concentration in the soil on uptake by terrestrial vascular plants. *Water Air Soil Pollut.* **80**, 1113–1116 (1995).
46. Juillerat, J. I., Ross, D. S. & Bank, M. S. Mercury in litterfall and upper soil horizons in forested ecosystems in Vermont, USA. *Environ. Toxicol. Chem.* **31**, 1720–1729 (2012).
47. Obrist, D., Johnson, D. W. & Edmonds, R. L. Effects of vegetation type on mercury concentrations and pools in two adjacent coniferous and deciduous forests. *J. Plant Nutr. Soil Sci.* **175**, 68–77 (2012).
48. Laacouri, A., Nater, E. A. & Kolka, R. K. Distribution and uptake dynamics of mercury in leaves of common deciduous tree species in Minnesota, USA. *Environ. Sci. Technol.* **47**, 10462–10470 (2013).
49. Lodenius, A., Tulisalo, E. & Soltanpour-Gargari, A. Exchange of mercury between atmosphere and vegetation under contaminated conditions. *Sci. Total. Environ.* **304**, 169–174 (2003).
50. Fay, L. & Gustin, M. Assessing the influence of different atmospheric and soil mercury concentrations on foliar mercury concentrations in a controlled

environment. *Water Air Soil Pollut.* **181**, 373–384 (2007).
51. Niu, Z. et al. Field controlled experiments on the physiological responses of maize (*Zea mays* L.) leaves to low-level air and soil mercury exposures. *Environ. Sci. Pollut. Res.* **21**, 1541–1547 (2014).
52. Assad, M. et al. Mercury uptake into poplar leaves. *Chemosphere* **146**, 1–7 (2016).
53. Millhollen, A. G., Gustin, M. S. & Obrist, D. Foliar mercury accumulation and exchange for three tree species. *Environ. Sci. Technol.* **40**, 6001–6006 (2006).
54. Mao, Y., Li, Y., Richards, J. & Cai, Y. Investigating uptake and translocation of mercury species by sawgrass (*Cladium jamaicense*) using a stable isotope tracer technique. *Environ. Sci. Technol.* **47**, 9678–9684 (2013).
55. Graydon, J. A. et al. Investigation of uptake and retention of atmospheric Hg(II) by boreal forest plants using stable Hg isotopes. *Environ. Sci. Technol.* **43**, 4960–4966 (2009).
56. Cui, L. W. et al. Accumulation and translocation of (198)Hg in four crop species. *Environ. Toxicol. Chem.* **33**, 334–340 (2014).
57. Yuan, W. et al. Stable isotope evidence shows re-emission of elemental mercury vapor occurring after reductive loss from foliage. *Environ. Sci. Technol.* **53**, 651–660 (2019).
Shows odd-MIF isotope fractionation during photochemical reduction and re-emission from foliage.
58. Olson, C. L., Jiskra, M., Sonke, J. E. & Obrist, D. Mercury in tundra vegetation of Alaska: Spatial and temporal dynamics and stable isotope patterns. *Sci. Total Environ.* **660**, 1502–1512 (2019).
59. Sun, L., Lu, B., Yuan, D., Hao, W. & Zheng, Y. Variations in the isotopic composition of stable mercury isotopes in typical mangrove plants of the Jiulong estuary, SE China. *Environ. Sci. Pollut. Res.* **24**, 1459–1468 (2017).
60. Graydon, J. A. et al. The role of terrestrial vegetation in atmospheric Hg deposition: Pools and fluxes of spike and ambient Hg from the METAALICUS experiment. *Global Biogeochem. Cycles* **26**, GB1022 (2012).
61. Rutter, A. P. et al. Dry deposition of gaseous elemental mercury to plants and soils using mercury stable isotopes in a controlled environment. *Atmos. Environ.* **45**, 848–855 (2011).
62. Bishop, K. H., Lee, Y. H., Munthe, J. & Dambrine, E. Xylem sap as a pathway for total mercury and methylmercury transport from soils to tree canopy in the boreal forest. *Biogeochemistry* **40**, 101–113 (1998).
Finds that 11% of the total Hg in litterfall was transported from soils to needles in xylem sap.
63. Beauford, W., Barber, J. & Barringer, A. Uptake and distribution of mercury within higher plants. *Physiol. Plant.* **39**, 261–265 (1977).
64. Cavallini, A., Natali, L., Durante, M. & Maserti, B. Mercury uptake, distribution and DNA affinity in durum wheat (*Triticum durum* Desf.) plants. *Sci. Total. Environ.* **243**, 119–127 (1999).
65. Blackwell, B. D. & Driscoll, C. T. Using foliar and forest floor mercury concentrations to assess spatial patterns of mercury deposition. *Environ. Pollut.* **202**, 126–134 (2015).
66. Amado Filho, G. M., Andrade, L. R., Farina, M. & Malm, O. Hg localisation in *Tillandsia usneoides* L. (Bromeliaceae), an atmospheric biomonitor. *Atmos. Environ.* **36**, 881–887 (2002).
67. Du, S.-H. & Fang, S. C. Catalase activity of C_3 and C_4 species and its relationship to mercury vapor uptake. *Environ. Exp. Botany* **23**, 347–353 (1983).
68. Leonard, T. L., Taylor, G. E., Gustin, M. S. & Fernandez, G. C. J. Mercury and plants in contaminated soils: 1. Uptake, partitioning, and emission to the atmosphere. *Environ. Toxicol. Chem.* **17**, 2063–2071 (1998).
69. Converse, A. D., Riscassi, A. L. & Scanlon, T. M. Seasonal variability in gaseous mercury fluxes measured in a high-elevation meadow. *Atmos. Environ.* **44**, 2176–2185 (2010).
70. Fritsche, J. et al. Elemental mercury fluxes over a sub-alpine grassland determined with two micrometeorological methods. *Atmos. Environ.* **42**, 2922–2933 (2008).
71. Fu, X. et al. Depletion of atmospheric gaseous elemental mercury by plant uptake at Mt. Changbai, Northeast China. *Atmos. Chem. Phys.* **16**, 12861–12873 (2016).
72. Manceau, A., Wang, J., Rovezzi, M., Glatzel, P. & Feng, X. Biogenesis of mercury–sulfur nanoparticles in plant leaves from atmospheric gaseous mercury. *Environ. Sci. Technol.* **52**, 3935–3948 (2018).
Reports the formation of stable Hg sulfur nanoparticles in foliage based on spectroscopy.
73. Carrasco-Gil, S. et al. Mercury localization and speciation in plants grown hydroponically or in a natural environment. *Environ. Sci. Technol.* **47**, 3082–3090 (2013).
74. Carrasco-Gil, S. et al. Complexation of Hg with phytochelatins is important for plant Hg tolerance. *Plant Cell Environ.* **34**, 778–791 (2011).
75. Niu, Z. et al. The linear accumulation of atmospheric mercury by vegetable and grass leaves: Potential biomonitors for atmospheric mercury pollution. *Environ. Sci. Pollut. Res.* **20**, 6337–6343 (2013).
76. Frescholtz, T. F., Gustin, M. S., Schorran, D. E. & Fernandez, G. C. J. Assessing the source of mercury in foliar tissue of quaking aspen. *Environ. Toxicol. Chem.* **22**, 2114–2119 (2003).
77. Zhou, J. et al. Mercury fluxes, budgets, and pools in forest ecosystems of China: A review. *Crit. Rev. Environ. Sci. Technol.* **50**, 1411–1450 (2020).
78. Gunda, T. & Scanlon, T. M. Topographical influences on the spatial distribution of soil mercury at the catchment scale. *Water Air Soil Pollut.* **224**, 1511 (2013).
79. Lindberg, S. E., Hanson, P. J., Meyers, T. P. & Kim, K. H. Air/surface exchange of mercury vapor over forests - The need for a reassessment of continental biogenic emissions. *Atmos. Environ.* **32**, 895–908 (1998).
80. Poissant, L., Pilote, M., Yumvihoze, E. & Lean, D. Mercury concentrations and foliage/atmosphere fluxes in a maple forest ecosystem in Québec, Canada. *J. Geophys. Res. Atmos.* **113**, D10307 (2008).
81. Ericksen, J. A. & Gustin, M. S. Foliar exchange of mercury as a function of soil and air mercury concentrations. *Sci. Total Environ.* **324**, 271–279 (2004).
82. Luo, Y. et al. Foliage/atmosphere exchange of mercury in a subtropical coniferous forest in south China. *J. Geophys. Res. Biogeosci.* **121**, 2006–2016 (2016).
83. Teixeira, D. C., Lacerda, L. D. & Silva-Filho, E. V. Foliar mercury content from tropical trees and its correlation with physiological parameters in situ. *Environ. Pollut.* **242**, 1050–1057 (2018).
84. Bacci, E., Gaggi, C., Duccini, M., Bargagli, R. & Renzoni, A. Mapping mercury vapours in an abandoned cinnabar mining area by azalea (*Azalea indica*) leaf trapping. *Chemosphere* **29**, 641–656 (1994).
85. Du, S. H. & Fang, S. C. Uptake of elemental mercury vapor by C_3 and C_4 species. *Environ. Exp. Botany* **22**, 437–443 (1982).
86. Battke, F., Ernst, D., Fleischmann, F. & Halbach, S. Phytoreduction and volatilization of mercury by ascorbate in *Arabidopsis thaliana*, European beech and Norway spruce. *Appl. Geochem.* **23**, 494–502 (2008).
87. Wohlgemuth, L. et al. A bottom-up quantification of foliar mercury uptake fluxes across Europe. *Biogeosciences* **17**, 6441–6456 (2020).
88. Ollerova, H., Maruskova, A., Kontrisova, O. & Pliestikova, L. Mercury accumulation in *Picea abies* (L.) Karst. needles with regard to needle age. *Pol. J. Environ. Stud.* **19**, 1401–1404 (2010).
89. Hutnik, R. J., McClenahen, J. R., Long, R. P. & Davis, D. D. Mercury accumulation in *Pinus nigra* (Austrian Pine). *Northeast. Nat.* **21**, 529–540 (2014).
90. Navratil, T. et al. Decreasing litterfall mercury deposition in central European coniferous forests and effects of bark beetle infestation. *Sci. Total Environ.* **682**, 213–225 (2019).
91. Hall, B. D. & Louis, V. L. S. Methylmercury and total mercury in plant litter decomposing in upland forests and flooded landscapes. *Environ. Sci. Technol.* **38**, 5010–5021 (2004).
92. Rasmussen, P. E., Mierle, G. & Nriagu, J. O. The analysis of vegetation for total mercury. *Water Air Soil Pollut.* **56**, 379–390 (1991).
93. Zhang, H. H., Poissant, L., Xu, X. H. & Pilote, M. Explorative and innovative dynamic flux bag method development and testing for mercury air–vegetation gas exchange fluxes. *Atmos. Environ.* **39**, 7481–7493 (2005).
94. Zhou, J., Wang, Z. W., Sun, T., Zhang, H. & Zhang, X. S. Mercury in terrestrial forested systems with highly elevated mercury deposition in southwestern China: The risk to insects and potential release from wildfires. *Environ. Pollut.* **212**, 188–196 (2016).
95. Clackett, S. P., Porter, T. J. & Lehnherr, I. 400-year record of atmospheric mercury from tree-rings in Northwestern Canada. *Environ. Sci. Technol.* **52**, 9625–9633 (2018).
96. Jung, R. & Ahn, Y. S. Distribution of mercury concentrations in tree rings and surface soils adjacent to a phosphate fertilizer plant in southern Korea. *Bull. Environ. Contam. Toxicol.* **99**, 253–257 (2017).
97. Kang, H. H. et al. Characterization of mercury concentration from soils to needle and tree rings of Schrenk spruce (*Picea schrenkiana*) of the middle Tianshan Mountains, northwestern China. *Ecol. Indic.* **104**, 24–31 (2019).
98. Navratil, T. et al. Larch tree rings as a tool for reconstructing 20th century Central European atmospheric mercury trends. *Environ. Sci. Technol.* **52**, 11060–11068 (2018).
99. Navratil, T. et al. The history of mercury pollution near the Spolana chlor-alkali plant (Neratovice, Czech Republic) as recorded by Scots pine tree rings and other bioindicators. *Sci. Total. Environ.* **586**, 1182–1192 (2017).
100. Schneider, L., Allen, K., Walker, M., Morgan, C. & Haberle, S. Using tree rings to track atmospheric mercury pollution in Australia: The legacy of mining in Tasmania. *Environ. Sci. Technol.* **53**, 5697–5706 (2019).
101. Wright, G., Woodward, C., Peri, L., Weisberg, P. J. & Gustin, M. S. Application of tree rings dendrochemistry for detecting historical trends in air Hg concentrations across multiple scales. *Biogeochemistry* **120**, 149–162 (2014).
102. Hojdova, M. et al. Changes in mercury deposition in a mining and smelting region as recorded in tree rings. *Water Air Soil Pollut.* **216**, 73–82 (2011).
103. Tangahu, B. V. et al. A review on heavy metals (As, Pb, and Hg) uptake by plants through phytoremediation. *Int. J. Chem. Eng.* **2011**, 939161 (2011).
104. Farella, N., Lucotte, M., Davidson, R. & Daigle, S. Mercury release from deforested soils triggered by base cation enrichment. *Sci. Total Environ.* **368**, 19–29 (2006).
105. Clemens, S. Toxic metal accumulation, responses to exposure and mechanisms of tolerance in plants. *Biochimie* **88**, 1707–1719 (2006).
106. Clemens, S. & Ma, J. F. Toxic heavy metal and metalloid accumulation in crop plants and foods. *Annu. Rev. Plant Biol.* **67**, 489–512 (2016).
107. Park, J. et al. The phytochelatin transporters AtABCC1 and AtABCC2 mediate tolerance to cadmium and mercury. *Plant J.* **69**, 278–288 (2012).
108. Wang, J. J. et al. Fine root mercury heterogeneity: metabolism of lower-order roots as an effective route for mercury removal. *Environ. Sci. Technol.* **46**, 769–777 (2012).
Reports that the estimated Hg return flux from dead, fine roots outweighed that from leaf litter, and ephemeral first-order roots that constituted 7.2–22.3% of total fine root biomass might have contributed the most to this flux.
109. Zhou, J. et al. Influence of soil mercury concentration and fraction on bioaccumulation process of inorganic mercury and methylmercury in rice (*Oryza sativa* L.). *Environ. Sci. Pollut. Res.* **22**, 6144–6154 (2015).
110. Yin, R., Feng, X. & Meng, B. Stable mercury isotope variation in rice plants (*Oryza sativa* L.) from the Wanshan mercury mining district, SW China. *Environ. Sci. Technol.* **47**, 2238–2245 (2013).
111. Wang, X. et al. Underestimated sink of atmospheric mercury in a deglaciated forest chronosequence. *Environ. Sci. Technol.* **54**, 8083–8093 (2020).
112. Rewald, B., Ephrath, J. E. & Rachmilevitch, S. A root is a root is a root? Water uptake rates of *Citrus* root orders. *Plant Cell Environ.* **34**, 33–42 (2011).
113. Balabanova, B., Stafilov, T., Sajn, R. & Andonovska, K. B. Quantitative assessment of metal elements using moss species as biomonitors in downwind area of lead-zinc mine. *J. Environ. Sci. Health A* **52**, 290–301 (2017).
114. Lopez Berdonces, M. A., Higueras, P. L., Fernandez-Pascual, M., Borreguero, A. M. & Carmona, M. The role of native lichens in the biomonitoring of gaseous mercury at contaminated sites. *J. Environ. Manage.* **186**, 207–213 (2017).
115. Pradhan, A. et al. Heavy metal absorption efficiency of two species of mosses (*Physcomitrella patens* and *Funaria hygrometrica*) studied in mercury treated culture under laboratory condition. *IOP Conf. Ser. Mater. Sci. Eng.* **225**, 012225 (2017).
116. Solberg, Y. & Selmerolsen, A. R. Studies on chemistry of lichens and mosses. 17. Mercury content of several lichen and moss species collected in Norway. *Bryologist* **81**, 144–149 (1978).

117. Stankovic, J. D., Sabovljevic, A. D. & Sabovljevic, M. S. Bryophytes and heavy metals: a review. *Acta Bot. Croat.* **77**, 109–118 (2018).
118. Hauck, M. & Runge, M. Occurrence of pollution-sensitive epiphytic lichens in woodlands affected by forest decline: a new hypothesis. *Flora* **194**, 159–168 (1999).
119. Salemaa, M., Derome, J., Helmisaari, H. S., Nieminen, T. & Vanha-Majamaa, I. Element accumulation in boreal bryophytes, lichens and vascular plants exposed to heavy metal and sulfur deposition in Finland. *Sci. Total Environ.* **324**, 141–160 (2004).
120. Lodenius, M. Dry and wet deposition of mercury near a chlor-alkali plant. *Sci. Total Environ.* **213**, 53–56 (1998).
121. Zechmeister, H. G., Hohenwallner, D., Riss, A. & Hanus-Illnar, A. Variations in heavy metal concentrations in the moss species *Abietinella abietina* (Hedw.) Fleisch according to sampling time, within site variability and increase in biomass. *Sci. Total Environ.* **301**, 55–65 (2003).
122. Bargagli, R. Moss and lichen biomonitoring of atmospheric mercury: A review. *Sci. Total Environ.* **572**, 216–231 (2016).
Highlights that cryptogams are good biomonitors of Hg natural/anthropogenic point sources, but estimates of air Hg concentrations and fluxes based on cryptogams are not reliable.
123. Wolterbeek, H. T. & Bode, P. Strategies in sampling and sample handling in the context of large-scale plant biomonitoring surveys of trace element air pollution. *Sci. Total Environ.* **176**, 33–43 (1995).
124. Wolterbeek, H. T., Garty, J., Reis, M. A. & Freitas, M. C. Biomonitors in use: lichens and metal air pollution. *Trace Metals Contam. Environ.* **6**, 377–419 (2003).
125. Dolegowska, S. & Migaszewski, Z. M. Plant sampling uncertainty: a critical review based on moss studies. *Environ. Rev.* **23**, 151–160 (2015).
126. Tyler, G. Bryophytes and heavy metals: a literature review. *Bot. J. Linn. Soc.* **104**, 231–253 (1990).
127. Onianwa, P. C. Monitoring atmospheric metal pollution: A review of the use of mosses as indicators. *Environ. Monit. Assess.* **71**, 13–50 (2001).
128. Wang, X., Yuan, W., Feng, X., Wang, D. & Luo, J. Moss facilitating mercury, lead and cadmium enhanced accumulation in organic soils over glacial erratic at Mt. Gongga, China. *Environ. Pollut.* **254**, 112974 (2019).
129. Vannini, A., Nicolardi, V., Bargagli, R. & Loppi, S. Estimating atmospheric mercury concentrations with lichens. *Environ. Sci. Technol.* **48**, 8754–8759 (2014).
130. Adamo, P. et al. Natural and pre-treatments induced variability in the chemical composition and morphology of lichens and mosses selected for active monitoring of airborne elements. *Environ. Pollut.* **152**, 11–19 (2008).
131. Bargagli, R. The elemental composition of vegetation and the possible incidence of soil contamination of samples. *Sci. Total Environ.* **176**, 121–128 (1995).
132. Bargagli, R. & Mikhailova, I. in *Monitoring with Lichens - Monitoring Lichens* Vol. 7 (eds Nimis, P. L., Scheidegger, P. L. & Wolseley, P. A.) 65–84 (Springer, 2002).
133. Nieboer, E. & Richardson, D. H. S. Lichens as monitors of atmospheric deposition. *Abstr. Pap. Am. Chem. Soc.* 146 (1979).
134. Walther, D. A. et al. Temporal changes in metal levels of the lichens *Parmotrema praesorediosum* and *Ramalina stenospora*, Southwest Louisiana. *Water Air Soil Pollut.* **53**, 189–200 (1990).
135. Garty, J. Biomonitoring atmospheric heavy metals with lichens: Theory and application. *Crit. Rev. Plant. Sci.* **20**, 309–371 (2001).
136. Nickel, S. et al. Modelling and mapping heavy metal and nitrogen concentrations in moss in 2010 throughout Europe by applying Random Forests models. *Atmos. Environ.* **156**, 146–159 (2017).
137. Harmens, H. et al. Mosses as biomonitors of atmospheric heavy metal deposition: Spatial patterns and temporal trends in Europe. *Environ. Pollut.* **158**, 3144–3156 (2010).
138. Frescholtz, T. F. & Gustin, M. S. Soil and foliar mercury emission as a function of soil concentration. *Water Air Soil Pollut.* **155**, 223–237 (2004).
139. Canario, J. et al. Salt-marsh plants as potential sources of Hg-0 into the atmosphere. *Atmos. Environ.* **152**, 458–464 (2017).
140. Graydon, J. A., St. Louis, V. L., Lindberg, S. E., Hintelmann, H. & Krabbenhoft, D. P. Investigation of mercury exchange between forest canopy vegetation and the atmosphere using a new dynamic chamber. *Environ. Sci. Technol.* **40**, 4680–4688 (2006).
141. Battke, F., Ernst, D. & Halbach, S. Ascorbate promotes emission of mercury vapour from plants. *Plant. Cell Environ.* **28**, 1487–1495 (2005).
142. Lindberg, S. E., Dong, W. J. & Meyers, T. Transpiration of gaseous elemental mercury through vegetation in a subtropical wetland in Florida. *Atmos. Environ.* **36**, 5207–5219 (2002).
143. Ericksen, J. A. et al. Accumulation of atmospheric mercury in forest foliage. *Atmos. Environ.* **37**, 1613–1622 (2003).
144. Fay, L. & Gustin, M. S. Investigation of mercury accumulation in cattails growing in constructed wetland mesocosms. *Wetlands* **27**, 1056–1065 (2007).
145. Agnan, Y., Le Dantec, T., Moore, C. W., Edwards, G. C. & Obrist, D. New constraints on terrestrial surface atmosphere fluxes of gaseous elemental mercury using a global database. *Environ. Sci. Technol.* **50**, 507–524 (2016).
Using available terrestrial surface–atmosphere Hg(0) flux studies reveals that, based on the current measurements available, global assimilation by vegetation cannot be determined appropriately with global flux uncertainty ranging from a net deposition of 513 Mg to a net emission of 1,353 Mg per year.
146. Sommar, J., Osterwalder, S. & Zhu, W. Recent advances in understanding and measurement of Hg in the environment: Surface-atmosphere exchange of gaseous elemental mercury (Hg^0). *Sci. Total Environ.* **721**, 137648 (2020).
147. Hanson, P. J., Lindberg, S. E., Tabberer, T. A., Owens, J. G. & Kim, K. H. Foliar exchange of mercury-vapor - evidence for a compensation point. *Water Air Soil Pollut.* **80**, 373–382 (1995).
148. Stamenkovic, J. et al. Atmospheric mercury exchange with a tallgrass prairie ecosystem housed in mesocosms. *Sci. Total Environ.* **406**, 227–238 (2008).
149. Zhou, J., Wang, Z., Zhang, X. & Sun, T. Investigation of factors affecting mercury emission from subtropical forest soil: a field controlled study in southwestern China. *J. Geochem. Explor.* **176**, 128–135 (2017).
150. Zhou, J., Wang, Z., Zhang, X., Driscoll, C. T. & Lin, C. J. Soil–atmosphere exchange flux of total gaseous mercury (TGM) at subtropical and temperate forest catchments. *Atmos. Chem. Phys.* **2020**, 16117–16133 (2020).
151. Bash, J. O. & Miller, D. R. Growing season total gaseous mercury (TGM) flux measurements over an *Acer rubrum* L. stand. *Atmos. Environ.* **43**, 5953–5961 (2009).
152. Fritsche, J. et al. Summertime elemental mercury exchange of temperate grasslands on an ecosystem-scale. *Atmos. Chem. Phys.* **8**, 7709–7722 (2008).
153. Lee, X., Benoit, G. & Hu, X. Z. Total gaseous mercury concentration and flux over a coastal saltmarsh vegetation in Connecticut, USA. *Atmos. Environ.* **34**, 4205–4213 (2000).
154. Slemr, F. et al. in *Proceedings of the 16th International Conference on Heavy Metals in the Environment* Vol. 1 (ed Pirrone, N.) 497 (E3S Web of Conferences, 2013).
155. Yuan, W. et al. Process factors driving dynamic exchange of elemental mercury vapor over soil in broadleaf forest ecosystems. *Atmos. Environ.* **219**, 117047 (2019).
156. Castro, M. S. & Moore, C. W. Importance of gaseous elemental mercury fluxes in western Maryland. *Atmosphere* **7**, 110 (2016).
157. Osterwalder, S. et al. Mercury evasion from a boreal peatland shortens the timeline for recovery from legacy pollution. *Sci. Rep.* **7**, 16022 (2017).
158. Yu, Q. et al. Gaseous elemental mercury (GEM) fluxes over canopy of two typical subtropical forests in south China. *Atmos. Chem. Phys.* **18**, 495–509 (2018).
159. Baya, A. P. & Van Heyst, B. Assessing the trends and effects of environmental parameters on the behaviour of mercury in the lower atmosphere over cropped land over four seasons. *Atmos. Chem. Phys.* **10**, 8617–8628 (2010).
160. Zhu, W., Sommar, J., Lin, C. J. & Feng, X. Mercury vapor air–surface exchange measured by collocated micrometeorological and enclosure methods–Part II: Bias and uncertainty analysis. *Atmos. Chem. Phys.* **15**, 5359–5376 (2015).
161. Blum, J. D., Sherman, L. S. & Johnson, M. W. Mercury isotopes in earth and environmental sciences. *Annu. Rev. Earth Planet. Sci.* **42**, 249–269 (2014).
162. Kwon, S. Y. et al. Mercury stable isotopes for monitoring the effectiveness of the Minamata Convention on Mercury. *Earth Sci. Rev.* **203**, 103111 (2020).
163. Enrico, M. et al. Atmospheric mercury transfer to peat bogs dominated by gaseous elemental mercury dry deposition. *Environ. Sci. Technol.* **50**, 2405–2412 (2016).
Proposes Δ^{200}Hg as a conservative tracer for atmospheric deposition pathways.
164. Gratz, L. E., Keeler, G. J., Blum, J. D. & Sherman, L. S. Isotopic composition and fractionation of mercury in Great Lakes precipitation and ambient air. *Environ. Sci. Technol.* **44**, 7764–7770 (2010).
165. Chen, J., Hintelmann, H., Feng, X. & Dimock, B. Unusual fractionation of both odd and even mercury isotopes in precipitation from Peterborough, ON, Canada. *Geochim. Cosmochim. Acta* **90**, 33–46 (2012).
166. Sherman, L. S., Blum, J. D., Keeler, G. J., Demers, J. D. & Dvonch, J. T. Investigation of local mercury deposition from a coal-fired power plant using mercury isotopes. *Environ. Sci. Technol.* **46**, 382–390 (2012).
167. Demers, J. D., Blum, J. D. & Zak, D. R. Mercury isotopes in a forested ecosystem: Implications for air-surface exchange dynamics and the global mercury cycle. *Global Biogeochem. Cycles* **27**, 222–238 (2013).
Demonstrates that dry deposition represents a major deposition pathway through the use of Hg stable isotopes.
168. Demers, J. D., Sherman, L. S., Blum, J. D., Marsik, F. J. & Dvonch, J. T. Coupling atmospheric mercury isotope ratios and meteorology to identify sources of mercury impacting a coastal urban-industrial region near Pensacola, Florida, USA. *Global Biogeochem. Cycles* **29**, 1689–1705 (2015).
169. Wang, Z. et al. Mass-dependent and mass-independent fractionation of mercury isotopes in precipitation from Guiyang, SW China. *C. R. Geosci.* **347**, 358–367 (2015).
170. Fu, X., Marusczak, N., Wang, X., Gheusi, F. & Sonke, J. E. Isotopic composition of gaseous elemental mercury in the free troposphere of the Pic du Midi observatory, France. *Environ. Sci. Technol.* **50**, 5641–5650 (2016).
171. Yu, B. et al. Isotopic composition of atmospheric mercury in China: new evidence for sources and transformation processes in air and in vegetation. *Environ. Sci. Technol.* **50**, 9262–9269 (2016).
172. Tsui, M. T. et al. Sources and transfers of methylmercury in adjacent river and forest food webs. *Environ. Sci. Technol.* **46**, 10957–10964 (2012).
173. Liu, H. -w. et al. Mercury isotopic compositions of mosses, conifer needles, and surface soils: Implications for mercury distribution and sources in Shergyla Mountain, Tibetan Plateau. *Ecotoxicol. Environ. Saf.* **172**, 225–231 (2019).
174. Jiskra, M. et al. Mercury deposition and re-emission pathways in boreal forest soils investigated with Hg isotope signatures. *Environ. Sci. Technol.* **49**, 7188–7196 (2015).
175. Zheng, W., Obrist, D., Weis, D. & Bergquist, B. A. Mercury isotope compositions across North American forests. *Global Biogeochem. Cycles* **30**, 1475–1492 (2016).
176. Woerndle, G. E. et al. New insights on ecosystem mercury cycling revealed by stable isotopes of mercury in water flowing from a headwater peatland catchment. *Environ. Sci. Technol.* **52**, 1854–1861 (2018).
177. Fu, X. et al. Significant seasonal variations in isotopic composition of atmospheric total gaseous mercury at forest sites in China caused by vegetation and mercury sources. *Environ. Sci. Technol.* **53**, 13748–13756 (2019).
178. Sun, R. et al. Modelling the mercury stable isotope distribution of Earth surface reservoirs: implications for global Hg cycling. *Geochim. Cosmochim. Acta* **246**, 156–173 (2019).
179. Wang, X. et al. Climate and vegetation as primary drivers for global mercury storage in surface soil. *Environ. Sci. Technol.* **53**, 10665–10675 (2019).
180. Biswas, A., Blum, J. D., Bergquist, B. A., Keeler, G. J. & Xie, Z. Q. Natural mercury isotope variation in coal deposits and organic soils. *Environ. Sci. Technol.* **42**, 8303–8309 (2008).
181. Guedron, S. et al. Mercury isotopic fractionation during pedogenesis in a tropical forest soil catena (French Guiana): Deciphering the impact of historical gold mining. *Environ. Sci. Technol.* **52**, 11573–11582 (2018).
182. Grasby, S. E. et al. Isotopic signatures of mercury contamination in latest Permian oceans. *Geology* **45**, 55–58 (2017).

183. Lepak, R. F. et al. Use of stable isotope signatures to determine mercury sources in the Great Lakes. *Environ. Sci. Technol. Lett.* **2**, 335–341 (2015).
184. Araujo, B. F., Hintelmann, H., Dimock, B., Almeida, M. G. & Rezende, C. E. Concentrations and isotope ratios of mercury in sediments from shelf and continental slope at Campos Basin near Rio de Janeiro, Brazil. *Chemosphere* **178**, 42–50 (2017).
185. Gleason, J. D. et al. Sources and cycling of mercury in the paleo Arctic Ocean from Hg stable isotope variations in Eocene and Quaternary sediments. *Geochim. Cosmochim. Acta* **197**, 245–262 (2017).
186. Masbou, J. et al. Hg-stable isotope variations in marine top predators of the Western Arctic Ocean. *ACS Earth Space Chem.* **2**, 479–490 (2018).
187. Fu, X. et al. Atmospheric wet and litterfall mercury deposition at urban and rural sites in China. *Atmos. Chem. Phys.* **16**, 11547–11562 (2016).
188. Wright, L. P., Zhang, L. & Marsik, F. J. Overview of mercury dry deposition, litterfall, and throughfall studies. *Atmos. Chem. Phys.* **16**, 13399–13416 (2016).
189. Zhang, L. et al. The estimated six-year mercury dry deposition across North America. *Environ. Sci. Technol.* **50**, 12864–12873 (2016).
Shows that GEM dry deposition over vegetated surfaces will not decrease, and, sometimes, might even increase with decreasing anthropogenic emissions.
190. Wang, X., Bao, Z. D., Lin, C. J., Yuan, W. & Feng, X. B. Assessment of global mercury deposition through litterfall. *Environ. Sci. Technol.* **50**, 8548–8557 (2016).
First study to estimate the global spatial distribution and budget of Hg dry deposition via plant Hg uptake using comprehensive litterfall data.
191. Dastoor, A. P. et al. Modeling dynamic exchange of gaseous elemental mercury at polar sunrise. *Environ. Sci. Technol.* **42**, 5183–5188 (2008).
192. Cooke, C. A., Martinez-Cortizas, A., Bindler, R. & Gustin, M. S. Environmental archives of atmospheric Hg deposition–A review. *Sci. Total Environ.* **709**, 134800 (2020).
193. Zhang, H., Holmes, C. D. & Wu, S. Impacts of changes in climate, land use and land cover on atmospheric mercury. *Atmos. Environ.* **141**, 230–244 (2016).
194. Melendez-Perez, J. J. et al. Soil and biomass mercury emissions during a prescribed fire in the Amazonian rain forest. *Atmos. Environ.* **96**, 415–422 (2014).
195. Richardson, J. B. & Friedland, A. J. Mercury in coniferous and deciduous upland forests in northern New England, USA: implications of climate change. *Biogeosciences* **12**, 6737–6749 (2015).
196. Yang, Y., Yanai, R. D., Driscoll, C. T., Montesdeoca, M. & Smith, K. T. Concentrations and content of mercury in bark, wood, and leaves in hardwoods and conifers in four forested sites in the northeastern USA. *PLoS ONE* **13**, e0196293 (2018).
197. Zhou, J., Wang, Z. W., Zhang, X. S. & Gao, Y. Mercury concentrations and pools in four adjacent coniferous and deciduous upland forests in Beijing, China. *J. Geophys. Res. Biogeosci.* **122**, 1260–1274 (2017).
198. Obrist, D. Atmospheric mercury pollution due to losses of terrestrial carbon pools? *Biogeochemistry* **85**, 119–123 (2007).
199. Demers, J. D., Driscoll, C. T., Fahey, T. J. & Yavitt, J. B. Mercury cycling in litter and soil in different forest types in the Adirondack region, New York, USA. *Ecol. Appl.* **17**, 1341–1351 (2007).
200. Heyes, A., Moore, T. R. & Rudd, J. W. M. Mercury and methylmercury in decomposing vegetation of a pristine and impounded wetland. *J. Environ. Qual.* **27**, 591–599 (1998).
201. Wang, X. et al. Enhanced accumulation and storage of mercury on subtropical evergreen forest floor: Implications on mercury budget in global forest ecosystems. *J. Geophys. Res. Biogeosci.* **121**, 2096–2109 (2016).
202. Zhou, J., Wang, Z. W. & Zhang, X. S. Deposition and fate of mercury in litterfall, litter, and soil in coniferous and broad-leaved forests. *J. Geophys. Res. Biogeosci.* **123**, 2590–2603 (2018).
203. Yuan, W. et al. Stable mercury isotope transition during postdepositional decomposition of biomass in a forest ecosystem over five centuries. *Environ. Sci. Technol.* **54**, 8739–8749 (2020).
204. Pokharel, A. K. & Obrist, D. Fate of mercury in tree litter during decomposition. *Biogeosciences* **8**, 2507–2521 (2011).
205. Lim, A. G. et al. A revised pan-Arctic permafrost soil Hg pool based on Western Siberian peat Hg and carbon observations. *Biogeosciences* **17**, 3083–3097 (2020).
206. Wright, L. P. & Zhang, L. An approach estimating bidirectional air-surface exchange for gaseous elemental mercury at AMNet sites. *J. Adv. Model Earth Syst.* **7**, 35–49 (2015).
207. Zhu, W. et al. Global observations and modeling of atmosphere–surface exchange of elemental mercury: a critical review. *Atmos. Chem. Phys.* **16**, 4451–4480 (2016).
Reviews the state of science in the atmosphere–surface exchange mechanisms, observation techniques and model parameterizations.
208. Wesely, M. L. & Hicks, B. B. A review of the current status of knowledge on dry deposition. *Atmos. Environ.* **34**, 2261–2282 (2000).
209. Christensen, J. H., Brandt, J., Frohn, L. M. & Skov, H. Modelling of mercury in the Arctic with the Danish Eulerian Hemispheric Model. *Atmos. Chem. Phys.* **4**, 2251–2257 (2004).
210. Dastoor, A. et al. Atmospheric mercury in the Canadian Arctic. Part II: Insight from modeling. *Sci. Total. Environ.* **509**, 16–27 (2015).
211. De Simone, F., Gencarelli, C. N., Hedgecock, I. M. & Pirrone, N. Global atmospheric cycle of mercury: a model study on the impact of oxidation mechanisms. *Environ. Sci. Pollut. Res.* **21**, 4110–4123 (2014).
212. Holmes, C. D., Jacob, D. J., Soerensen, A. L. & Corbitt, E. S. Global atmospheric budget of mercury including oxidation of Hg(0) by bromine atoms. *Geochim. Cosmochim. Acta* **74**, A413–A413 (2010).
213. Travnikov, O. & Ilyin, I. in *Mercury Fate and Transport in the Global Atmosphere* (eds Pirrone, N. & Mason, R.) 571–587 (Springer, 2009).
214. Kerkweg, A. et al. An implementation of the dry removal processes DRY DEPosition and SEDImentation in the Modular Earth Submodel System (MESSy). *Atmos. Chem. Phys.* **6**, 4617–4632 (2006).
215. Wesely, M. L. & Lesht, B. M. Comparison of RADM dry deposition algorithms with a site-specific method for inferring dry deposition. *Water Air Soil Pollut.* **44**, 273–293 (1989).
216. Zhang, L., Brook, J. & Vet, R. A revised parameterization for gaseous dry deposition in air-quality models. *Atmos. Chem. Phys.* **3**, 2067–2082 (2003).
217. Zhang, L., Wright, L. P. & Blanchard, P. A review of current knowledge concerning dry deposition of atmospheric mercury. *Atmos. Environ.* **43**, 5853–5864 (2009).
218. Huang, J., Miller, M. B., Edgerton, E. & Gustin, M. S. Deciphering potential chemical compounds of gaseous oxidized mercury in Florida, USA. *Atmos. Chem. Phys.* **17**, 1689–1698 (2017).
219. Travnikov, O. et al. Multi-model study of mercury dispersion in the atmosphere: atmospheric processes and model evaluation. *Atmos. Chem. Phys.* **17**, 5271–5295 (2017).
Reviews global Hg models and their differences, uncertainties and evaluation with measurements.
220. Bash, J. O., Miller, D. R., Meyer, T. H. & Bresnahan, P. A. Northeast United States and Southeast Canada natural mercury emissions estimated with a surface emission model. *Atmos. Environ.* **38**, 5683–5692 (2004).
221. Durnford, D. et al. How relevant is the deposition of mercury onto snowpacks?–Part 2: A modeling study. *Atmos. Chem. Phys.* **12**, 9251–9274 (2012).
222. Fisher, L. S. & Wolfe, M. H. Examination of mercury inputs by throughfall and litterfall in the Great Smoky Mountains National Park. *Atmos. Environ.* **47**, 554–559 (2012).
223. Gbor, P. K. et al. Improved model for mercury emission, transport and deposition. *Atmos. Environ.* **40**, 973–983 (2006).
224. Lin, C. J., Lindberg, S. E., Ho, T. C. & Jang, C. Development of a processor in BEIS3 for estimating vegetative mercury emission in the continental United States. *Atmos. Environ.* **39**, 7529–7540 (2005).
225. Selin, N. E. et al. Global 3-D land-ocean-atmosphere model for mercury: Present-day versus preindustrial cycles and anthropogenic enrichment factors for deposition. *Global Biogeochem. Cycles* **22**, GB2011 (2008).
226. Shetty, S. K., Lin, C.-J., Streets, D. G. & Jang, C. Model estimate of mercury emission from natural sources in East Asia. *Atmos. Environ.* **42**, 8674–8685 (2008).
227. Smith-Downey, N. V., Sunderland, E. M. & Jacob, D. J. Anthropogenic impacts on global storage and emissions of mercury from terrestrial soils: Insights from a new global model. *J. Geophys. Res. Biogeosci.* **115**, G03008 (2010).
228. Xu, X. H., Yang, X. S., Miller, D. R., Helble, J. J. & Carley, R. J. Formulation of bi-directional atmosphere-surface exchanges of elemental mercury. *Atmos. Environ.* **33**, 4345–4355 (1999).
229. Bash, J. O. Description and initial simulation of a dynamic bidirectional air-surface exchange model for mercury in Community Multiscale Air Quality (CMAQ) model. *J. Geophys. Res. Atmos.* **115**, D06305 (2010).
Describes the most comprehensive scheme for modelling bidirectional Hg exchange fluxes over the vegetation canopy by defining dynamic compensation points based on partitioning coefficients across air–foliage and air–soil surfaces.
230. Wang, X., Lin, C. J. & Feng, X. Sensitivity analysis of an updated bidirectional air–surface exchange model for elemental mercury vapor. *Atmos. Chem. Phys.* **14**, 6273–6287 (2014).
231. Lin, C.-J. et al. Scientific uncertainties in atmospheric mercury models I: Model science evaluation. *Atmos. Environ.* **40**, 2911–2928 (2006).
232. Graydon, J. A. et al. Investigation of uptake and retention of atmospheric Hg(II) by boreal forest plants using stable Hg isotopes. *Environ. Sci. Technol.* **43**, 4960–4966 (2009).
233. Zhang, H. et al. Assessing air–surface exchange and fate of mercury in a subtropical forest using a novel passive exchange-meter device. *Environ. Sci. Technol.* **53**, 4869–4879 (2019).
234. Khan, T. R., Obrist, D., Agnan, Y., Selin, N. E. & Perlinger, J. A. Atmosphere-terrestrial exchange of gaseous elemental mercury: parameterization improvement through direct comparison with measured ecosystem fluxes. *Environ. Sci. Process. Impacts* **21**, 1699–1712 (2019).
Demonstrates that the use of resistance-based models combined with the new soil re-emission flux parameterization is able to reproduce observed diel and seasonal patterns of Hg(0) exchange in these ecosystems.
235. Dastoor, A. P. & Larocque, Y. Global circulation of atmospheric mercury: a modelling study. *Atmos. Environ.* **38**, 147–161 (2004).
236. Fraser, A., Dastoor, A. & Ryjkov, A. How important is biomass burning in Canada to mercury contamination? *Atmos. Chem. Phys.* **18**, 7263–7286 (2018).
237. Kos, G. et al. Evaluation of discrepancy between measured and modelled oxidized mercury species. *Atmos. Chem. Phys.* **13**, 4839–4863 (2013).
238. Angot, H. et al. Global and local impacts of delayed mercury mitigation efforts. *Environ. Sci. Technol.* **52**, 12968–12977 (2018).
239. Kwon, S. Y. & Selin, N. E. Uncertainties in atmospheric mercury modeling for policy evaluation. *Curr. Pollut. Rep.* **2**, 103–114 (2016).
240. Vorholt, J. Microbial life in the phyllosphere. *Nat. Rev. Microbiol.* **10**, 828–840 (2012).
241. Cole, A. et al. Ten-year trends of atmospheric mercury in the high Arctic compared to Canadian sub-Arctic and mid-latitude sites. *Atmos. Chem. Phys.* **13**, 1535–1545 (2013).
242. Gay, D. A. et al. The Atmospheric Mercury Network: measurement and initial examination of an ongoing atmospheric mercury record across North America. *Atmos. Chem. Phys.* **13**, 11339–11349 (2013).
243. Tørseth, K. et al. Introduction to the European Monitoring and Evaluation Programme (EMEP) and observed atmospheric composition change during 1972–2009. *Atmos. Chem. Phys.* **12**, 5447–5481 (2012).
244. Sprovieri, F. et al. Atmospheric mercury concentrations observed at ground-based monitoring sites globally distributed in the framework of the GMOS network. *Atmos. Chem. Phys.* **16**, 11915–11935 (2016).
245. Custodio, D., Ebinghaus, R., Spain, T. G. & Bieser, J. Source apportionment of atmospheric mercury in the remote marine atmosphere: Mace Head GAW station, Irish western coast. *Atmos. Chem. Phys.* **20**, 7929–7939 (2020).
246. Slemr, F. et al. Atmospheric mercury in the Southern Hemisphere–Part 1: Trend and inter-annual variations in atmospheric mercury at Cape Point, South Africa, in 2007–2017, and on Amsterdam Island in 2012–2017. *Atmos. Chem. Phys.* **20**, 7683–7692 (2020).
247. Slemr, F. et al. Comparison of mercury concentrations measured at several sites in the Southern Hemisphere. *Atmos. Chem. Phys.* **15**, 3125–3133 (2015).

248. Howard, D. et al. Atmospheric mercury in the Southern Hemisphere tropics: seasonal and diurnal variations and influence of inter-hemispheric transport. *Atmos. Chem. Phys.* **17**, 11623–11636 (2017).
249. McLagan, D. S. et al. Global evaluation and calibration of a passive air sampler for gaseous mercury. *Atmos. Chem. Phys.* **18**, 5905–5919 (2018).
250. Liu, Z. et al. A review on phytoremediation of mercury contaminated soils. *J. Hazard. Mater.* **400**, 123138 (2020).
251. Anjum, N. A., Duarte, A. C., Pereira, E. & Ahmad, I. *Juncus maritimus* root biochemical assessment for its mercury stabilization potential in Ria de Aveiro coastal lagoon (Portugal). *Environ. Sci. Pollut. Res.* **22**, 2231–2238 (2015).
252. Shehu, J. et al. Hyperaccumulators of mercury in the industrial area of a PVC factory in Vlora (Albania). *Arch. Biol. Sci.* **66**, 1457–1463 (2014).
253. Qian, X. et al. Total mercury and methylmercury accumulation in wild plants grown at wastelands composed of mine tailings: Insights into potential candidates for phytoremediation. *Environ. Pollut.* **239**, 757–767 (2018).
254. Pogrzeba, M. et al. *Dactylis glomerata* L. cultivation on mercury contaminated soil and its physiological response to granular sulphur aided phytostabilization. *Environ. Pollut.* **255**, 113271 (2019).
255. Moreno, F. N. et al. Effect of thioligands on plant-Hg accumulation and volatilisation from mercury-contaminated mine tailings. *Plant Soil* **275**, 233–246 (2005).
256. Rascio, N. & Navari-Izzo, F. Heavy metal hyperaccumulating plants: How and why do they do it? And what makes them so interesting? *Plant Sci.* **180**, 169–181 (2011).
257. Wang, J. et al. Ammonium thiosulphate enhanced phytoextraction from mercury contaminated soil–Results from a greenhouse study. *J. Hazard. Mater.* **186**, 119–127 (2011).
258. Franchi, E. et al. Phytoremediation of a multi contaminated soil: mercury and arsenic phytoextraction assisted by mobilizing agent and plant growth promoting bacteria. *J. Soil. Sediment.* **17**, 1224–1236 (2017).
259. Smolinska, B. The influence of compost and nitrilotriacetic acid on mercury phytoextraction by *Lepidium sativum* L. *J. Chem. Technol. Biotechnol.* **95**, 950–958 (2020).
260. Wang, J. et al. Thiosulphate-induced phytoextraction of mercury in *Brassica juncea*: Spectroscopic investigations to define a mechanism for Hg uptake. *Environ. Pollut.* **242**, 986–993 (2018).
261. Fan, Y. et al. Phytoextraction potential of soils highly polluted with cadmium using the cadmium/zinc hyperaccumulator *Sedum plumbizincicola*. *Int. J. Phytoremediation* **21**, 733–741 (2019).

Acknowledgements
We would like to thank X. Wang and C.-J. Lin for providing us with Hg litterfall deposition fluxes and biome geospatial boundary masks that allowed us to compare model results with litterfall deposition for various biomes of the world. We thank the three anonymous reviewers for their constructive comments on an earlier version of this manuscript. Funding was provided by the US National Science Foundation (AGS award no. 1848212 and DEB award no. 2027038). M.J. acknowledges funding from the Swiss National Science Foundation grant PZ00P2_174101. We thank James Gray for editorial comments on the manuscript.

Author contributions
All authors contributed to the writing, editing and overall conceptualization of this review manuscript. J.Z. built and analyzed the database, and led the writing of the manuscript and overall design of graphics and tables. D.O. initiated and coordinated the project and co-led manuscript writing and editing. A.D. led the model approach, analysis and associated sections. A.R. built the modelling set-up and conducted simulations, analysis and associated graphics. M.J. led the sections on stable Hg isotope patterns, data collection and analysis, and associated graphics.

Competing interests
The authors declare no competing interests.

Peer review information
Nature Reviews Earth & Environment thanks Charles Driscoll, Karin Eklof and the other, anonymous, reviewer(s) for their contribution to the peer review of this work.

Publisher's note
Springer Nature remains neutral with regard to jurisdictional claims in published maps and institutional affiliations.

Supplementary information
The online version contains supplementary material available at https://doi.org/10.1038/s43017-021-00146-y.